CZECH TECHNICAL UNIVERSITY IN PRAGUE

FACULTY OF MECHANICAL ENGINEERING

DEPARTMENT OF MECHANICS, BIOMECHANICS AND MECHATRONICS

AUTHOR **Bc. Adéla Kováříková**

SUPERVISOR **Ing. Jakub Kronek, PhD.**

Prague 2019

ZADÁNÍ DIPLOMOVÉ PRÁCE

I. OSOBNÍ A STUDIJNÍ ÚDAJE

Příjmení: **Kovářiková** Jméno: **Adéla** Osobní číslo: **437083**

Fakulta/ústav: **Fakulta strojní**

Zadávající katedra/ústav: **Ústav mechaniky, biomechaniky a mechatroniky**

Studijní program: **Strojní inženýrství**

Studijní obor: **Biomechanika a lékařské přístroje**

II. ÚDAJE K DIPLOMOVÉ PRÁCI

Název diplomové práce:

Vliv vyvažování kolenní náhrady na její životnost

Název diplomové práce anglicky:

Knee prosthesis balancing and its impact on lifetime

Pokyny pro vypracování:

Vyvažování kolenních náhrad je snahou o nalezení optimální polohy komponent náhrady v těle pacienta, aby byly oba kondyly femorální komponenty zatěžovány přibližně stejně a zůstávaly stále v kontaktu s tibiální vložkou (nedocházelo k cyklickému 'narážení' dílů o sebe). Technika empiricky funguje, chybí ovšem biomechanický vhled do problematiky, např. jaká míra nevyvážení kolene je ještě přípustná a neovlivní negativně opotřebení a tím pádem i životnost náhrady. Student provede rešerši problematiky s důrazem na mechaniku tohoto systému (kontaktní tlaky, otěr), navrhne systém přípravků pro nastavení nevyvážení a upnutí náhrady do otěrového simulátoru a v laboratoři biotribologie provede otěrový experiment s vyváženou a nevyváženou náhradou. Výstupem práce bude míra opotřebení v obou případech, jakožto tvarová změna artikulačních ploch náhrad. Diplomová práce bude vypracována ve spolupráci s firmou Beznoska s.r.o.

Seznam doporučené literatury:

1) Babazadeh, S., Stoney, J.D., Lim, K. et al. The relevance of ligament balancing in total knee arthroplasty: how important is it? A systematic review of the literature. Orthopedic Reviews. 2009; 1: e26
2) Jawhar, A., Hutter, K., Scharf, HP. Outcome in total knee arthroplasty with a medial-lateral balanced versus unbalanced gap. J Orthop Surg (Hong Kong) 2016;24:298-301.

Jméno a pracoviště vedoucí(ho) diplomové práce:

Ing. Jakub Kronek, Ph.D., ústav mechaniky, biomechaniky a mechatroniky FS

Jméno a pracoviště druhé(ho) vedoucí(ho) nebo konzultanta(ky) diplomové práce:

Datum zadání diplomové práce: **25.04.2019** Termín odevzdání diplomové práce: **16.08.2019**

Platnost zadání diplomové práce: _____

Ing. Jakub Kronek, Ph.D.	prof. Ing. Milan Růžička, CSc.	prof. Ing. Michael Valášek, DrSc.
podpis vedoucí(ho) práce	podpis vedoucí(ho) ústavu/katedry	podpis děkana(ky)

III. PŘEVZETÍ ZADÁNÍ

Diplomantka bere na vědomí, že je povinna vypracovat diplomovou práci samostatně, bez cizí pomoci, s výjimkou poskytnutých konzultací. Seznam použité literatury, jiných pramenů a jmen konzultantů je třeba uvést v diplomové práci.

30.4.2019

Datum převzetí zadání

Podpis studentky

Anotation Page

Author	Bc. Adéla Kováříková
Czech Title	Vliv vyvažování kolenní náhrady na její životnost
English Title	Knee prosthesis balancing and its impact on lifetime
Year	2019
Course of Study	Biomechanics and Medical Devices
Department	Department of Mechanics, Biomechanics and Mechatronics
Supervisor	Ing. Jakub Kronek, PhD.

Bibliographic Figures

Number of Pages: 72

Number of Figures: 37

Number of Tables: 9

Klíčová slova

Kolenní náhrada, vyvažování, simulátor, metoda konečných prvků, tribologie, tibiální vložka, kontaktní tlak

Keywords

Knee Implant, Ligament Balancing, Simulator, Finite Element Method, Tribology, Tibial Insert, Contact pressure

Anotace

Cílem této práce je posouzení vlivu vyvažování kolenních náhrad na jejich životnost. Je testován MKP model tibiální vložky ve vyváženém a nevyváženém stavu a proveden otěrový experiment tibiální vložky v obou stavech. Ze skenů artikulačních ploch je vyhodnocen rozdíl lineárního otěru ve vyváženém a nevyváženém stavu.

Abstract

The aim of this thesis is to evaluate the impact of ligament balancing on implant lifetime. A FE model of the tibial insert was tested in a balanced and unbalanced state and a wear test of the tibial insert in both states was conducted. The change in linear wear was evaluated from scans of articulating surfaces in the balanced and unbalanced state.

Declaration of Honor

I declare, that I wrote this thesis on my own with the help of my supervisor. All used literature is properly cited and stated in the References.

In Prague, ……

Adéla Kováříková

Acknowledgments

I would like to thank my supervisor Ing. Jakub Kronek, PhD. for his time, support and help with my Diploma Thesis. I would also like to thank Danny Pincivero, who helped me with my literature research at the University of Waterloo and everyone at Mecas Esi for allowing me to do a part of this thesis as an internship.

A big thank you goes to my family and friends who have been patient with me and have supported me throughout my studies.

Content

List of Used Symbols

Symbol	Units	Meaning
μ	[Pa*s]	Dynamic Viscosity
N	[mm/s]	Entrainment Speed
W_n	[mm]	Linear Wear Depth
k_A	[m^2/N]	Archards constant
P	[MPa]	Contact Pressure
S	[mm]	Sliding Distance
D	[mm]	Wire Diameter
De	[mm]	External Spring Diameter
Lo	[mm]	Free Length of Spring
Ln	[mm]	Compressed Length of Spring
w	[mm]	Width of the Tibial Component

List of Used Abreviations

TKR	Total Knee Replacement
ACL	Anterior Cruciate Ligament
PCL	Posterior Cruciate Ligament
LCL	Lateral Collateral Ligament
MCL	Medial Collateral Ligament
RMS	Root Mean Square

Introduction

Total knee replacement (TKR) has evolved to become one of the most important and frequent orthopedic surgeries since its' origin in the middle of the 20th century, with around 16000 knee replacements performed every year in the Czech Republic and this number is expected to rise to 28000-30000 [1]. With an increasing number of people suffering from arthrosis and knee damage caused by injuries, it is necessary to be able to provide a solution for these patients. They are often in pain and the bone damage to their knee joint is so severe it affects their everyday movement, preventing them from enjoying their regular activities. With the replacement of their knee using a modern implant, they can often resume most of their previously abandoned activities of daily living. Although the knee joint prosthesis field has evolved immensely in the past 70 years, there are still limitations to improve. Implants can get infected and not properly integrate in the body, requiring the patients to go trough revision surgery, which makes up for 20 % of all TKR's in the Czech Republic [2]. The common causes for revision are implant loosening, infection, wear and instability. This does not only increase the cost of the surgery, but most importantly puts the patient through even more discomfort. Further enhancements should therefore be done in the material and construction aspect of implants.

The aim of my research project is to investigate the effect of implant balancing on its' wear and lifetime. This process of releasing and resecting ligaments follows the removal of osteophytes (bone projections along the joint) and menisci. It currently mostly relies on the surgeons' experience. It is considered one of the key parts of a successful knee replacement, because it ensures a balanced and stable knee without asymmetrical medial or lateral gaps and helps recover full mobility of the joint. The improper balancing could lead to tighter medial/lateral ligaments, resulting in higher contact pressure and wear on one of the condyles. This would not only mean the reoccurence of a valgus/varus deformity, but higher wear rates lead to shorter implant lifetimes and needs for further reoperations. Proper ligament balancing can therefore prolong the lifetime of the implant, reduce the risk of reoperations, lower the costs and provide a smooth experience for the patient.

In the theoretical part, I will present fundamental facts about the knee anatomy and its' biomechanics. Implant types and materials will also be discussed before the topic of ligament balancing is introduced and explained. The fundamentals of wear tribology will be presented, since the linear wear of the knee implant will be evaluated.

The practical part will consist of two parts. A finite element model simulation of the knee implant will be conducted in the balanced and unbalanced state. Contact pressure and linear wear depth will be evaluated. Then two tibial inserts will be tested in the wear simulator, with one of them being exposed to an added spring to simulate the unbalanced knee.

Theoretical Part

2.1 The Knee Joint Anatomy

The knee (articulatio genus, figure 1) is the largest and most complex joint in the human body. It is a modified hinge joint which permits front plane motion during flexion and extension. The knee consists of two articulations – a tibiofemoral and a patellofemoral. [3]

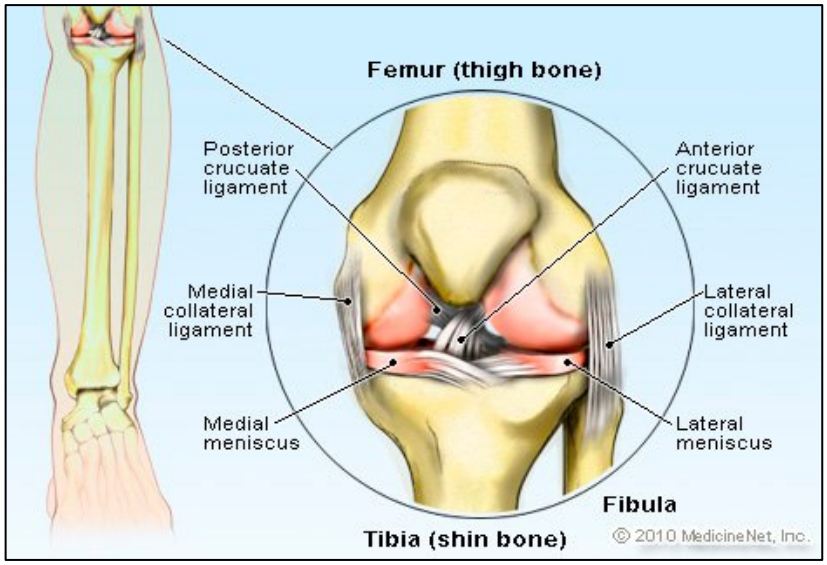

Figure 1: Anatomy of the Knee Joint [4]

2.1.1 Patella

The patella is a bone in the tendon insertion area of musculus (m.) quadriceps femoris. The anterior patellar area (facies anterior) is part of this tendon, while its posterior part (facies posterior) is covered in cartilage and is adjacent to facies patellaris femoris of the femur. [3]

2.1.2 Femur

The femur (os femoris) is the longest and most massive bone in the body. The proximal part consists of a round head (caput femoris) which is part of the hip joint. The distal part, that articulates in the knee is made of two rounded bulges – the medial and lateral condyles. [3]

2.1.3 Tibia

The tibia has a wider proximal part which interacts with the femur in the tibiofemoral joint. This upper area consists of a medial and lateral condyle and together they form an area called facies articularis superior. The articular surface of the medial condyle is elliptical and hollow, while the surface of the lateral condyle is smaller and flat. Between these two condyles lies an elevation eminentia intercondylaris. [3]

2.1.4 Articular capsule

The articular capsule (figure 2) is structurally complicated and variously indented in its' fibrous and synovial layer.

The fibrous layer is attached at the tibia and patella on the edges of their articular surfaces and at the femur around 1–1.5 cm from its joint surfaces. The capsule does not cover femoral epicondyles where muscles and ligaments insert. [3, 5]

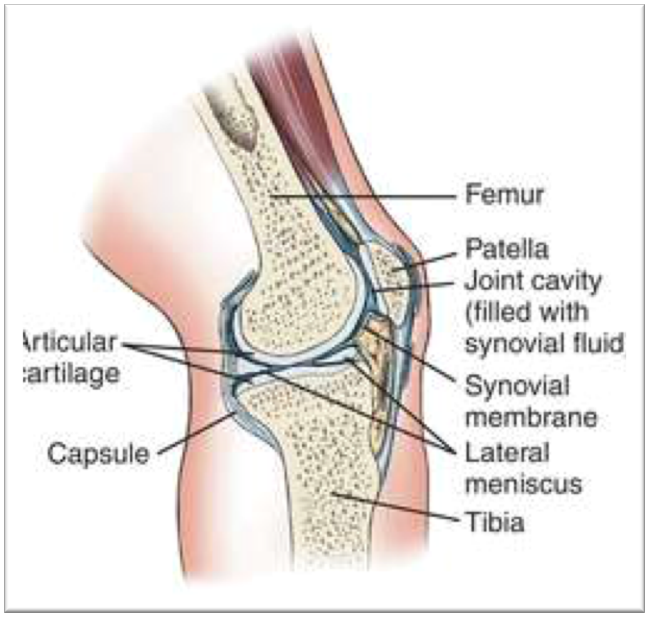

Figure 2: Knee joint [6]

2.1.5 Ligaments

Ligaments of the knee articulation can be divided into two groups – ligaments of the knee capsule and interarticular ligaments. Knee capsule ligaments can also be separated into anterior, posterior and collateral ligaments.

- Anterior knee capsule ligaments

The tendon of musculus quadriceps femoris inserts at the patella and continues as the patellar ligament, which goes from the patella to tibial tuberosity. Apex patellae is embedded in this ligament. [3]

Fibrous bands along the sides of the patella, that go from m. quadriceps femoris to the tibia, are called retinaculum patellae mediale et laterale. The lateral retinaculum is also strengthened by the connection to tractus iliotibialis. [3]

- Posterior knee capsule ligaments

Ligamentum popliteum obliquum is located lateroproximaly along the posterior side of the knee capsule. It is not a real joint ligament, but rather the continuation of the tendon of musculus semimembranosus. [3]

The fibular side includes the ligamentum popliteum arcuatum that creates an open arch in its proximal part. This arch is convex and produces fibrous bands from its convexities that go to caput fibulae. This structure resembles the letter "Y". [3]

- Collateral knee ligaments

Ligamentum collaterale tibiale is wide and flat and in its posterior part connected via the knee capsule with the medial meniscus. It begins on the medial epicondyle of the femur and inserts at the tibia approximately 6-9 mm under the knee cleft. This ligament is completely stretched during knee extension where it stabilises the knee. [3]

Ligamentum collaterale fibulare forms a rounded fascicle that sticks out of the knee capsule, because of the fat tissue and blood vessels that are positioned between the ligament and capsule in the knee cleft area. This ligament is on the lateral side of the knee and goes from the lateral epicondyle femoris to the back of caput fibulae (1 cm under the top). It is completely stretched during knee extension. [3]

- Intraarticular ligaments

Ligamentum cruciatum anterius attaches at the medial area of the lateral femoral condyle inserts at the anterior intercondylar are of the tibia. [3]

Ligamentum cruciatum posterius goes from the outter area of the medial femoral condyle to the area intecondylaris posterior tibia. It crosses the anterior cruciate ligament at its back. [3]

Cruciate ligaments ensure the stability of the knee, especially during flexion, when they stretch. The also limit the possible knee rotation by twisting. The ACL limits anterior tibial movement and ensures medial rotation of the shank. It is maximally loaded during medial rotation, especially when the knee is in hyperextension. PCL limits posterior tibial movement and lateral rotation. [3]

Ligamentum transversum genus is incorporated in the knee capsule and plica infrapatellaris and connects both of the menisci. [3]

Ligamentum meniscofemorale posterius et anterius fixate the posterior tip of the lateral meniscus. They are located around the posterior and anterior face of the posterior cruciate ligament and insert at the medial femoral condyle. [3]

2.1.6 Menisci

The contact between articular surfaces of the femur a tibia wouldn't be ideal, because the curvature of the femur condyles is bigger, and its shape does not respond to the proximal tibial articular surfaces. To prevent this, two menisci (figure 3) exist. Both menisci are formed peripherally by dense fibrous tissue which continues into fibrocartilage. They are higher along their outer perimeter and very thin along the inner perimeter. During movement they move to the front and back while changing their shape at the same time. The medial and lateral meniscus differ in both shape and size. [3, 5]

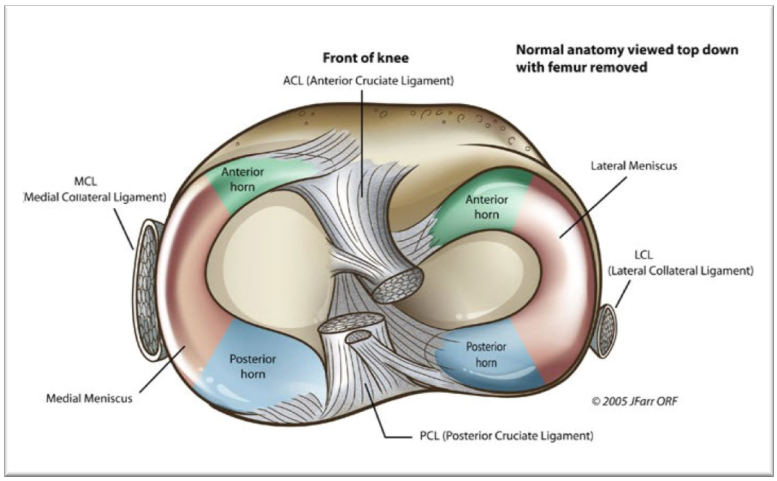

Figure 3: Front of the Knee view with menisci and Cruciate ligaments [7]

2.1.7 Bursae mucosae

Bursas are small sacks which are lined by synovial tissue and contain liquid. They are located (figure 4) in areas of friction and pressure and some of them communicate with thearticular cavity. [3]

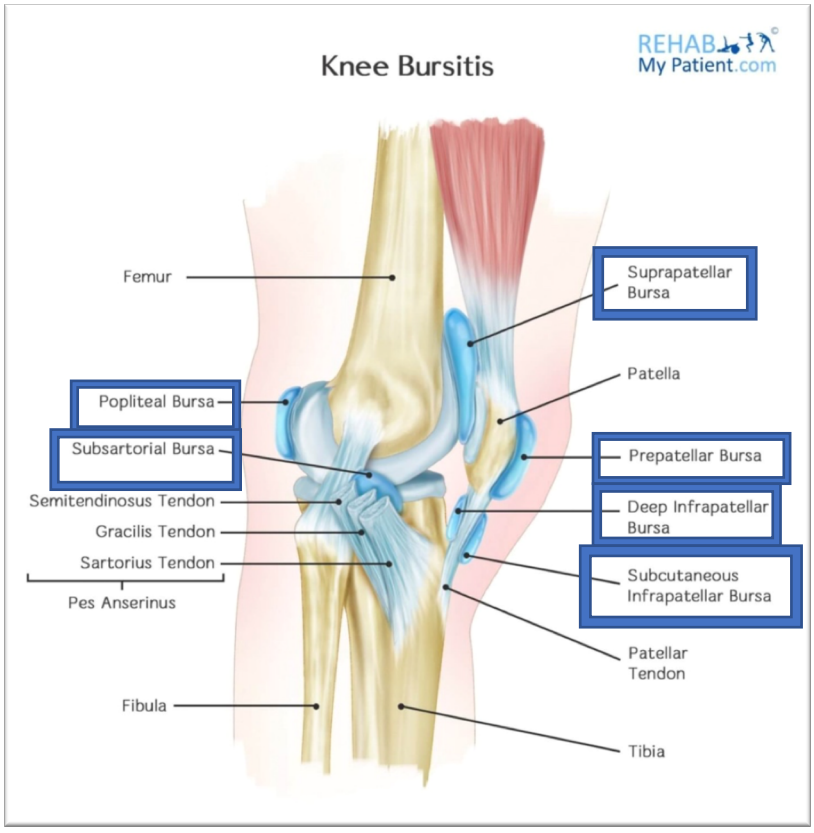

Figure 4: Knee Bursae [8]

2.1.8 Muscles of the knee joint

The knee joint is affected by muscles of the thigh, shank and two pelvic muscles that also contribute to the stabilisation (figure 5).

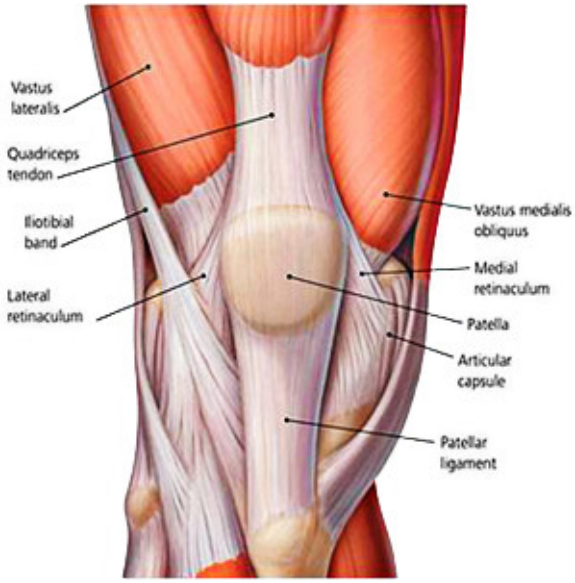

Figure 5: Muscles of the Knee [9]

2.1.8.1 Thigh muscles

- Ventral group

Musculus sartorius (figure 6) begins at spina iliaca anterior superior and ends at the pes anserinus. M. sartorius takes part in knee flexion and internal rotation while in flexion. [3]

Musculus quadriceps femoris is formed by four muscles. The longest of these is m. rectus femoris which starts at the spina iliaca anterior inferior of the pelvic bone. All three other muscles origin at the femur and and almost completely cover it. They are called – m. vastus medialis, lateralis and intermedius. All four muscles connect above the patella and terminate at the patella. They are important for knee extension. [3]

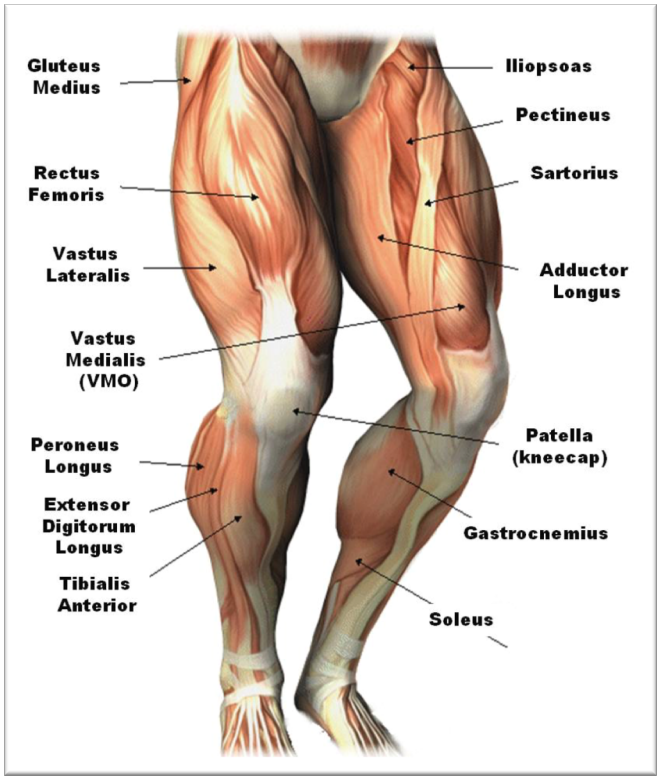

Figure 6: Muscles of the thigh and shank [10]

- Medial group

The only muscle from the medial group that affects the knee joint is *musculus gracilis*. M. gracilis helps with flexion and rotation while the knee is flexed. [3]

- Dorsal group

Musculus biceps femoris has two heads – caput longum and caput breve. Biceps femoris is responsible for flexion and external rotation in flexion. [3]

Musculus semimembranosus has a flat tendon throughout almost half of his length. M. semimembranosus takes part in flexion and internal rotation while in flexion. [3]

Musculus semitendinosus begins at tuber ischiadicum and inserts through pes anserinus under the medial tibial condyle. This muscle takes part in knee flexion and internal rotation in flexion. [3]

2.1.8.2 Shank muscles

- Surface layer

Musculus triceps surae has two surface parts (m. gastrocnemius) and a deep part (m. soleus). Between these two layers we can find musculus plantaris. M. triceps surae helps with knee flexion, especially via m. gastrocnemius. [3]

- Deep layer

Musculus popliteus is the only deep muscle that affects the knee Musculus popliteus helps with knee flexion and internal rotation when in flexion. [3]

2.1.8.3 Pelvic muscles

Musculus gluteus maximus (figure 7) is the most important muscle for hip extension Gluteus maximus helps fixate knee extension through pulling on the tractus iliotibialis. [3]

Musculus tensor fascie latae affects the knee joint through tractus tibialis as well. It takes part in knee rotaion and also fixates knee extension when standing. [3]

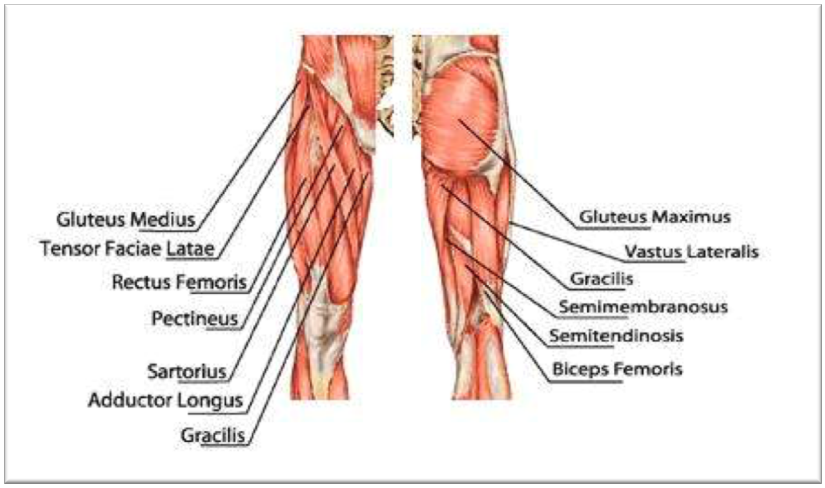

Figure 7: Muscles of the hip and pelvis [11]

2.2 Biomechanics of the Knee Joint

Biomechanics of the knee joint not only depend on femur loading, but also on the muscle forces produced by surrounding muscles. The maximum force load in the initial step phase is approximately 2400 N for normal gait and 4000 N when walking down stairs. [15]

The knee joints responsibility is to ensure sufficient range of movement without the loss of stability in dynamic (walking, running, rotation) and static (standing) positions. These

functions are maintained through correct interaction between articular surfaces, ligaments, menisci and surrounding muscles. Injuries or imbalances in these structures can cause biomechanical changes and imbalanced loading of the joint. [16]

The combination of specific femoral and tibial articular surfaces with the ligament system provides the knee joint with six degrees of freedom (figure 8). Three degrees in rotation and three in translation movements. The basic active movements of the knee joint are flexion, extension, internal and external rotation. Other movements such as tibial/femoral anterior and posterior translation and abduction/adduction through varus/valgus forces are passive. The flexible connection and stability of the femoral and tibial part of the joint are ensured mostly by the cruciate ligaments. [17, 18, 19]

The degrees of freedom of a knee joint are described by osteokinematics, while the motion inside the joint is called arthokinematics. [19]

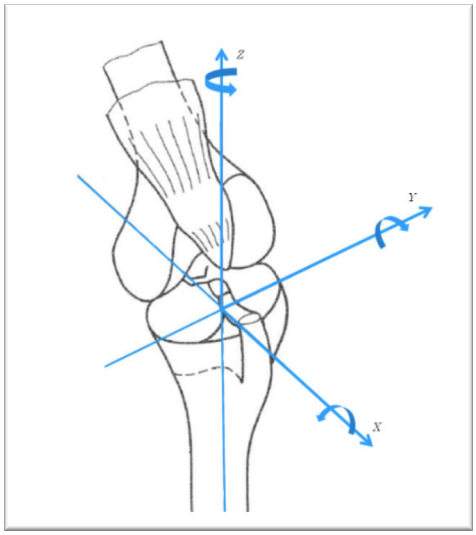

Figure 8: Degrees of freedom of the knee joint [20]

2.2.1 Flexion and Extension

The primary movements of the knee joint are flexion and extension. The maximal possible flexion varies according to different authors. According to Bartoníček [21], the maximal flexion is 160°, but the maximal active flexion is just 140°. The other 20° percent can be achieved through passive movement only. Russe [22] presents the active range of motion as just 130°. Norkin [18] states, that the passive range of motion is 130°-140°, while knee flexion might be limited to 120° only and might also reach up to 160°. [23]

Three movements are combined in flexion and extension with a fixed tibia [23, 24]:

- Initial rotation at the beginning of flexion and terminal rotation at the end of extension
- Rolling movement of femoral condyles along the anterior tibial plateau
- Slipping movement of femoral condyle posteriorly along the tibial plateau

The arrangement of knee ligaments and the specific shape of articular surfaces is the cause of these different motions. Based on this, it is clear that there is no permanent motion axis. [21, 23, 25]

Cruciate ligaments play a major part in coordinating all three movements, but especially in rolling and slipping. This coordination is essential for motion due to the different sized femoral and tibial condyles. If an injury of one of the cruciate ligaments occurs, the ratio between knee joint movements changes and allows more rolling. Patients with ACL lesions even show tribological changes due to the changed ratio between rolling and slipping motions. This causes premature joint wear. Collateral ligaments also help the knee resist hyperextension. [21, 22, 23]

Knee joint flexion is initiated by the internal rotation of the tibia (or external rotation of femur) by approximately 5° during the first 15° of flexion. The range of rotation is individual between 5°-20°. This motion is affected by [21, 23, 26]:

- Uneven profile and size of femoral condyles
- Uneven shape of tibial articular surfaces
- Uneven direction of fibres of collateral ligaments

The rotation process is controlled by ACL tension, its' tear or elongation does not prevent this movement, but does affect the center of rotation. Further flexion continues with rolling and slipping motions, their ratio does change with time and slipping becomes prevalent. [4, 21]

The contact between the tibia and the femur keeps getting smaller and the menisci slide dorsally along the tibia in the final stage of flexion. The movement of the lateral meniscus along the tibia is much bigger (approx. 12 mm) compared to the medial meniscus (6 mm). [23, 25]

During extension the motions happen in opposite order up to the terminal rotation, which then locks the extended knee.

2.2.2 Rotation

The range of rotation depends on the amount of knee flexion. Rotation is almost impossible during full extension because of the tension in most ligaments. The range widens with gradual flexion, mostly during the first 30°. The biggest range of motion occurs between 45°- 90° of flexion. The range of internal rotation is about 17° and external 21°. The axial pressure does also have a big impact on the range of rotation and decreases is by half in comparison to an unloaded joint. [21, 23, 26]

Rotation is mostly affected by the alignment of ligaments, whereas articular surfaces have very low impact. The ligaments can be divided into three groups [4, 21, 23]:

- Central group = cruciate ligaments
- Medial group = medial collateral ligament and joint capsule
- Lateral group = lateral collateral ligament and joint capsule

Through this structural arrangement, the femoral condyles are stabilised on both sides. Another very important factor is the cruciate ligament crossing in the frontal plane. While the PCL runs almost vertically, the angle of the ACL is much steeper. This provides greater motion space for the lateral femoral condyle opposed to the medial condyle. We also have to consider the different mobility of the menisci. The rotation kinematics depends on the location of the center of rotation. Most authors place this point to the external edge of the medial tubercle of the intercondylar eminence. [14, 21, 23, 26]

The external rotation range of the lower leg is mostly affected by collateral ligament tension. The ACL takes part in the terminal phase of movements, while the PCL does influence the movement minimally due to its close position to the center of rotation. [21]

Internal shank rotation is impacted by the lateral collateral ligament as well as the ACL, which is called the primary stabiliser by some authors, because of its crossing in the frontal plane. Internal rotation is also affected by the lateral meniscus and the posterolateral part of the joint capsule. [23, 26]

2.2.3 ACL tension

The ACL tension is not constant during knee movements. During full extension, the ACL is fully stretched. At 15° flexion the tension starts to go down and reaches its' minimum at approximately 30°- 40° flexion. With further flexion, the tension starts to grow again, so that at 90° its anteromedial part is strongly stretched. Through external rotation the

ACL tension relaxes, it only starts to tense again in extremal positions. Internal rotation causes the ligament to stretch noticeably. [14, 21, 23, 26]

2.2.4 Knee joint stability

The stability of the knee joint is maintained by three stabilisation systems [21]:

- Ligament stabilisation (passive, static)
- Muscle (active, dynamic) stabilisation and their control system
- Stability though the contact of articular surfaces (affected by the shape of surfaces and pressure forces of the knee)

Stability also depends on the extent of flexion and possible rotation of the joint. Maximal stability is during full extension, where most static stabilszers stretch – cruciate ligaments, both collateral ligaments, joint capsule, and dynamic stabilisers are also stretched. [21, 26]

2.2.5 Ligament stabilisation

The static stabilisation system consists of ligaments and most instabilites of the knee joint are connected to ligament damage. Ligaments must have a sufficient strength to ensure proper stabilisation and mobility. Ligament weakness, which can be caused by congenital or aquired factors, causes knee instability and weakness in the knee joint. The form of instability increases with the number of damaged ligaments. Injured crucial ligaments allow more shifting of the tibia in the sagittal plane. Knee instability is often caused by a combination of factors such as the laxity of crucial/collateral ligaments, a flacid joint capsule and possible menisci damage. [19, 21, 23, 28]

The ACL stabilises the anterior side of the tibia during passive movements. The effect of the ACL grows with the increasing range of motion. A Lachmann test can be conducted to diagnose a potential ACL injury. [21]

2.2.6 Dynamic stabilisers

Muscles around the knee joint form the active or dynamic stabilisation system. They key to their correct function is the neuromotoric control of the dynamic stabilisation and its' retrospective control. [23, 29]

Patients with soft tissue injuries regularly show changes in coordination and timing of stabilisation muscles, such as slower reaction times, slower achievement of the optimal moment of force and the disruption of anticipation mechanisms. [23]

For the dynamic support of ACL function the activation of hamstrings is required first, followed by mm. vasti and mm. gastrocnaemii. The hamstring preactivation is significant and takes up to 40 % of the stabilisation during the correction of the anterior tibial translation. These remarks clarify the idea that hamstrings are the agonist to the ACL. [29]

The balanced activation of medial and lateral hamstrings is also very important for correct stabilisation. The muscles must be activated sufficiently and on time. Higher activation on the m. biceps femoris side destabilises the knee especially against forces that internally rotate the femur against the tibia. This situation occurs often during long-term ACL insufficiency and after ACL replacement with a graft (m. semitendinosus/ m. gracilis). [29, 30]

The activation of m. vastus medialis and m. vastus lateralis is also important. The knee is stabilised by mm. gastrocnaemii as well. This muscle group pulls the femur dorsaly against the tibia while compressing the joint at the same time. The coactivation with mm. vasti is crucial for this function. [23, 31]

2.3 Knee Implants

2.3.1 Historical Review

The first knee implant was a hinge joint invented by Börje Waldius in 1951. The fixed connection between the femoral and tibial part did allow movement in the sagittal plane. Waldius first used an implant made from acryl and later replaced this by using a metal similar to vitalium. His knowledge was later used by Shierse and Young who modified his invention. [33]

Since the hinge implant did not respect the physiological knee motion, the forces acting on both bones were much higher and thus the implant got loose and caused further bone damage. This is therefore not used anymore today, unless it is specifically required – for example in patients with bone tumors. Hinge joints were adjusted to decrease the bone forces and they do not require as invasive bone resections as before. The construction is based on joints with low friction and with polyethylene contact surfaces. The disadvantage of this joint is its' complicated structure, which is at higher risk of damage. [34]

Further development later led to the invention of condylar implants which use thin components which imitate the physiological shape of the tibia and femur. This construction allows almost full range of movement, but it is crucial that collateral ligaments are preserved during the procedure. First condylar implants used simple geometric shapes such

as Gunston's implant. This model was not used for very long, because the contact forces were accumulating under the implant in the tibia and the implant became loose. A more advanced version was Freeman – Swanson's implant which had two modifications – one was used for crucial ligaments retaining procedure, while the other did not require the presence of the ligaments. [33, 34]

The most popular prosthesis in the 80's was the Geomedic implant, that was invented by Coventry et al. which ensures good range of motion and necessary rotation and stability. It required the complete preservation of all knee ligaments and the femoral component did not have a patellar contact surface. The femoral component was further enhanced to achieve better rotation and flexion by reducing the curvature of femoral condyles and later on the patellar surface was also added. The material used for the femoral part was a metal (Co or Ti alloy) and high molecular polyethylene was used for the tibia. [33, 34]

One of the first „modern "implants that included the tibial plateau was invented by Insall in 1974. A metal rod was inserted which provided a more even force distribution at the proximal tibial end and therefore improved the properties of the tibial component. Thanks to this, the indications for surgery were expanded to joints with big insufficiencies or complete crucial ligaments defects. [33,34]

The condylar implant was further improved by Insall, Lachiewiz and Bumstein to a dorsally stabilised model in 1979. Their femoral implant had a transversal cam which enabled knee flexion to up to 120°. Another anatomical implant was introduced by Howmedica and was called Townley. Menisci implants were invented in the 1980's. They provided translation and rotation movements in a similar range to the knee joint. These implants are very complicated structure wise and therefore difficult to manufacture, which lead to their high price. [33, 34]

2.4 Materials used in Knee Implants

The requirements for knee implant materials are very high and strict. They must have very good strenght and friction properties and of course be biocompatible. This means that they must be tolerated inside the human body and be resilient to it. Also, they must have high corrosion resistance not only to the material itself, but also to any products that might be produced due to friction. It is important to realise, that the introduction of a new material or new production technology requires a long-term testing process, which includes testing

the product on animal models. The most used materials in implants are metals and metal alloys, ceramics and plastics. [36, 37]

2.4.1 Ceramic materials

A ceramic implant using aluminium oxide was first produced in Japan in the 1980's. The benefit of ceramics in comparison to metals is their hardness and pressure strength. They can also achieve very smooth surfaces, have high resistance against abrasion and are greatly tolerated by the human body. Their disadvantages include fragility, low fracture resistance and complicated manufacturing where it is very difficult to reproduce more implants in a series. The most used ceramics materials are aluminium oxide Al_2O_3 and zirconium oxide ZrO_2. [38, 39]

2.4.2 Metal materials

Metals and metal alloys are frequently used for knee joint implants. They have very convenient mechanical properties, which can be adapted to specific needs, and they can also be altered using various technologies. Their chemical properties vastly depend on the atomic bonds and the mechanical properties are established by the crystallographic structure. [37, 38]

Pure metals themselves do usually not meet the requirements for implants, so they are altered by adding other components and creating alloys. The most significant alloys used in knee implants are Cr-Ni-Mo, Co-Cr-Mo and various Ti alloys. [37]

2.4.3 Plastic materials

Plastic materials are organic macromolecular materials (polymers). They usually contain additives to help achieve better properties. They can be divided into low molecular polymers with low molecular weights and high molecular polymers with high molecular weight. These weights determine their mechanical, physical and chemical properties. Polymers used throughout the history include: polytetrafluorethylene PTEE, polyester PET, polyethylene PE, polymethylmethacrylate PMMA (bone cement) and polyetheretherketone PEEK. PTEE and PET were not used for very long due to their unsatisfying integration inside the body, so most used ones are PE and PMMA. PEEK has been primarily used for spinal implants, but recent projects have introduced PEEK-based knee joints. This material has similar properties to natural bones and is cheaper and lighter compared to metals. [33, 38, 40]

2.4.4 UHMWPE

Bearing surfaces of joint replacements (figure 9) are usually made of ultrahigh molecular weight polyethylene (UHMWPE). It is currently the most efficient material in terms of mechanical properties, biocompatibility and wear resistence, although UHMWPE wear is still one of the most frequent reasons behind implant failures. [41]

Figure 9: UHMWPE tibial insert [42]

The properties of UHMWPE highly depend on its‘ processing and post-processing. These can positively affect the material and increase its‘ wear resistence and oxidation stability. In order to preserve a high purity in materials used for medical purposes, modifications cannot include further chemical additives. To achieve better properties, ionization, thermal modification, stabilisation with vitamin E and sterilization are frequently used. Cross-linking of UHMWPE leads to higher molecular weights and wear resistence, but slighty worse mechanical parameters such as strength and ductility. Four generations of UHMWPE are currently known. The density of cross-links is affected by the irradiation dose, for lower densities it is up to 40 kGy, whereas 50–100 kGy is used for highly cross-linked UHMWPE. [41, 43]

1. The 1st generation does not include any significant modifications except for sterilization by gamma-irradiation with doses of 25–45 kGy. [41]
2. The 2nd generation is modified by using higher doses (50–100 kGy) of radiation. After that, thermal modification to eliminate residual radicals and improve unwanted oxidation takes place and is followed by sterilization using ethylene oxide or gas plazma. The 2nd generation is also called highly cross-linked UHMWPE. [41]

3. The 3rd generation improves mechanical and oxidative properties of the 2nd generation by sequential irradiation or vitamin E stabilisation. Vitamin E is a natural antioxidant. It is a non-polar substance which can be dissolved in other non-polar materials such as UHMWPE. Therefore, it doesn't tend to unbind from the UHMWPE. Thermal treatment is not always present. [41, 43]
4. The 4th generation focuses on preserving the crystalline structure and properties of ultra high molecular UHMWPE while retaining the oxidative stability during irradiation. The incorporation of antioxidants neutralizes the free radicals present in the polyethylene without the need for further thermal melting. [44]

2.5 Types of knee joint implants

Knee joint implants can be divided by several criteria. One of them is the implantation criteria, which depends on how the implant is attached. These implants can be cemented or uncemented.

2.5.1 Cemented implants

These implants are attached to the bone using bone cement PMMA (poly methylmethacrylate). This method was first established in 1980. Their disadvantages compared to the uncemented implants (figure 10) are less bone stock preservation, possible cement debris and slower bone integration. A study of 400 total knee replacements was conducted to compare cemented and uncemented implants. The cemented group of 200 TKR's had 8 revision surgeries, 5 of these due to aseptic loosening (2.5 %). The uncemented group had 7 revisions with only one being due to aseptic loosening (3.5 %). [45, 46]

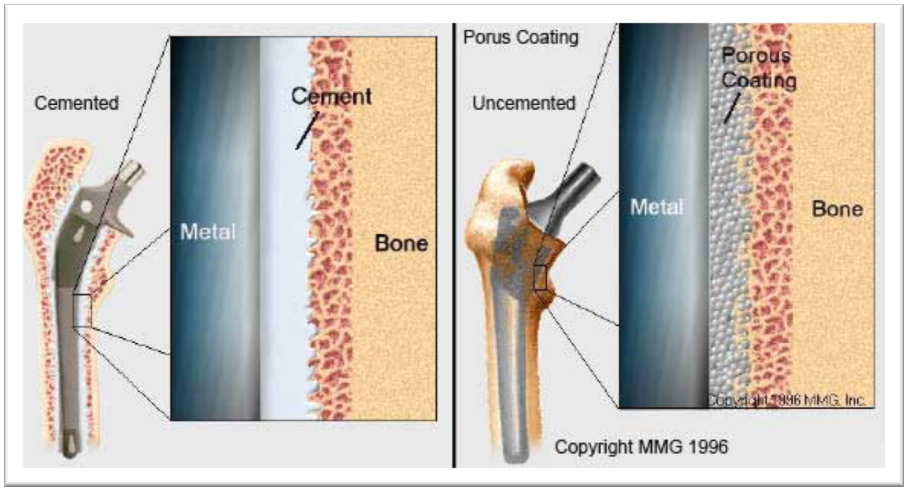

Figure 10: The difference between cemented and cementless implants [47]

2.5.2 Uncemented implants

In uncemented implants, the connection between the components and the bone is created without the use of bone cement. This method was invented in the 1980's. Since 1996 cementless implants with hydroxyapatite coatings are used. One of the technologies used is the Porous Coated Arthroplasty. The implant surface is covered with small macroscopic pores through which bone can grow and thereby fixate the implant. Another possibility is the use of bioactive ceramics, which include particles that can actively take part in bone growth. Usually it is a combination of mechanical and chemical bonds, where the bioactive ceramic is applied via coating onto the porous surface. For example, collagen surface coatings are being modified to include antibiotics, which are then being continuously released after implantation to prevent possible infects. A study, which investigated the adherence of a newly developed collagen, hydroxyapatite and antibiotics surface coat on titanium implants, showed good results after extrusion tests. [45, 49, 50]

Another differentiation criterion is the construction type. Here we distinguish between hinge implants, condylar implants and unicondylar implants.

2.5.3 Hinge implants

The connection between the tibial and femoral components is usually maintained by a pivot. Original constructs allowed only flexion-extension movement (figure 11). The benefit of this is a higher internal stability which is necessary in cases, where the knee deformity is high and often accompanied by axis instability. Latest models include a rotating hinge which also permits rotation. Revision surgeries are also often conducted by using hinge implants. Its' implantation requires more bone resection than other types which could lead to a higher risk of complications. [51, 52]

Figure 11: Hinge Knee Implant [53]

2.5.4 Condylar implants

In condylar implants (figure 12), the tibial and femoral components aren't attached to each other and therefore the knee can move in all planes. The implantation requires minimal bone resection and for cemented implants less PMMA is needed in comparison to hinge implants. Condylar implants are often produced in two options. The first one is "standard" and requires for both cruciate ligaments to be preserved. It also has pyramid protrusions, which should help with fixation. The second option is called total and has a central eminence on the tibial component. It compensates for the removed cruciate ligaments to some extent. It has a "I" shaped shaft for fixation in addition to protrusions. [51, 52]

Figure 12: Condylar Knee Prosthesis [54]

2.5.5 Unicondylar implants

In cases where only one condyle is damaged, unicondylar implants (figure 13) can be used. They require even less bone resection, shorter surgery time and ensure a faster and easier rehabilitation process. A study investigating the reasons for revision surgeries of unicondylar implants showed, that 41 % of all revisions were for early failure. This failure was caused by the collapse of the tibial component in 45.5 % and infection in 18.25 %. The primary cause for late failure was aseptic loosening with 44 %. [55]

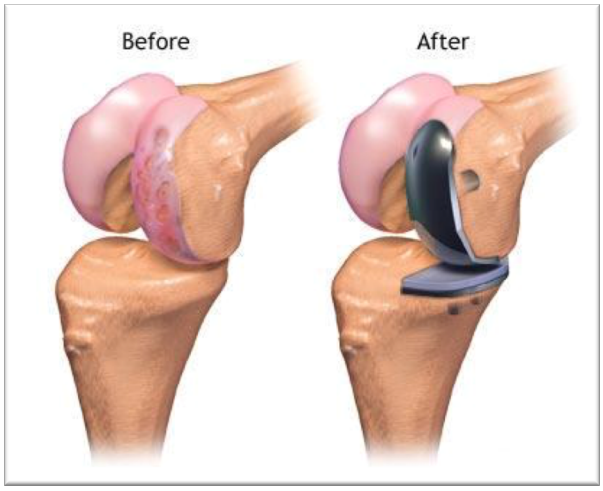

Figure 13: Visualisation of a Unicondylar Knee Implant [56]

2.6 Knee Replacement Surgery

Knee replacement surgery requires aseptic standards to be fulfilled, an equipped operating room and well-educated personnel. Reoperations caused by an infect can be technically challenging and costly. The patient is positioned on the back and the joint isentered using a longitudinal parapatellar cut. At first, the surgeon removes osteophytes, which are bone growths that cause ligament tightness and are one of the factors contributing to the need for TKR. The instruments for this surgery include special sizers which enable the surgeon to perform an exact bone resection using precalculated angles. After bone resection, trial implants are being placed and the knee joint motion is being tested to determine the best implant size. In this phase, the tension in static stabilisers is determined by releasing ligaments and surrounding tissue. The goal is to achieve symmetrical balance and tension. The fixation of implant components is possible with bone cement, or if the patient's bone quality is sufficient, an implant with porous surface can be inserted and osseointegration happens naturally.

2.7 Ligament Balancing

Ligament balancing is considered to be the key element to a successful knee replacement surgery. The process relies mostly on the surgeon's knowledge and practise and has a big impact on the post-operative range of movement of the affected knee joint. The positive result of a total knee replacement surgery is a balanced knee, which has the following attributes [57]:

- Full range of movement

- No varus/valgus deformities in flexion or extension
- Well balanced flexion/extension gap without any ligament tightness or laxity
- Symmetrical medial/lateral balance at 90° flexion and full extension
- Correct alignment of the patella
- Reduced patella during maximal flexion and no extra rollback of the femur on the tibia
- Balanced rotation between femoral and tibial components

Through the replacement of a knee joint, we are trying to recover the patients range of motion and alleviate pain caused by arthrosis. This process involves cartilage damage, the growth of osteophytes and joint deformations, which usually lead to a varus/valgus deformation. A knee with a bigger lateral gap and a deformed medial condyle is considered a varus knee. In this case both legs create a characteristic O shape. Valgus deformity, where legs are in a X shape, is present in patients with higher lateral joint damage. Both of these conditions cause irreversible ligament tightness shortening/elongating on the collapsed/convex side. Osteophytes lead to ligament tightness and therefore movement restrictions. Through ligament (figure 14) balancing, we are trying to restore the knee to its' pre-arthritic state. This usually involves the removal of osteophytes and a dissection (elongation) of ligaments. [53, 54]

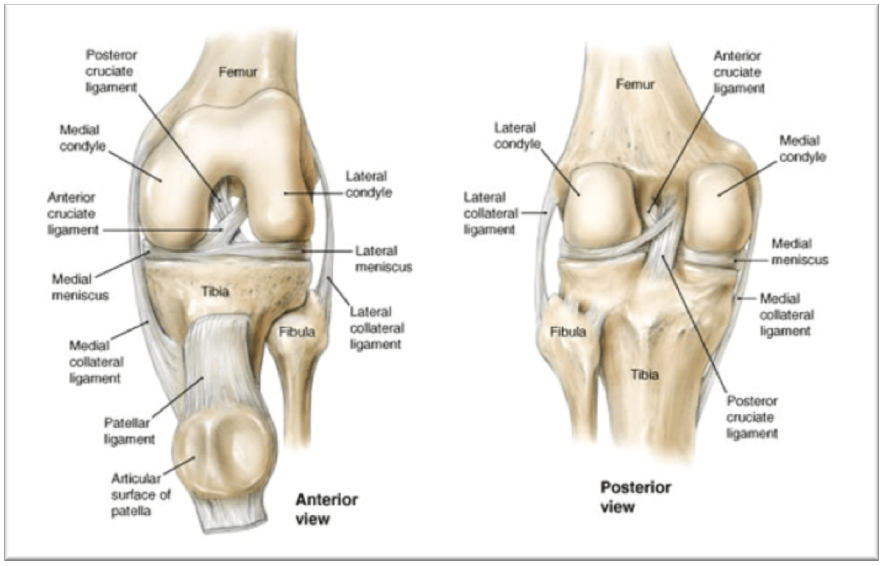

Figure 14: Deep Layer of Knee Ligaments [59]

Ligament balancing can have a positive influence on bone alignment, stability and prosthetic wear and loosening. A study showed, that implants that developed medial insert wear, which resulted in a varus deformity, did not have proper medial ligament

balancing. Not fully balancing a valgus knee can result in laxness of the medial collateral ligaments. These cannot tighten again with time and therefore the knee is likely to develop a valgus deformity again. Incorrect ligament balancing has been described as 27 % of all preventable revision surgeries performed due to instability. This issue is even more significant in cruciate retaining implants, where late failure of the PCL and a bigger flexion gap can lead to flexion instability. The same can be caused by a lax medial or lateral collateral ligament. A link between asymmetrical prosthesis wear and ligament balancing has also been proven. The reasons behind a higher wear can be improper ligament release or a too tight PCL. Balanced knees also have a higher success rate in terms of implant loosening, which is the most common cause for revisions (36.5 %). [56, 57, 60]

This is also linked with pain reduction. Post TKR pain is usually caused by wear, over-tight ligaments and instability, all of which can be improved by balancing. A study of 38 patients showed alleviated pain in patients with proper knee balancing. [61]

2.7.1 Ligament balancing techniques

There are two major techniques used to balance ligaments surrounding the knee (as shown in figures 14 and 15) during total knee replacement. Both begin with the removal of osteophytes and differ in the following process, where they can be divided into a “measured resection” and “balanced resection” technique. [57]

Using measured resection, the surgeon first performs the femoral/tibial cut and implant trial before he continues with the ligament balancing process. The amount of bone resection is predetermined using approximate calculations and should correspond to the implant thickness as well as to anatomical landmarks. Both of these cuts are performed separately using measuring devices. After this, the trial prosthesis is inserted and the knee is tested in flexion/extension with released ligaments. This should ensure a symmetrical gap and appropriate ligament tension. [57, 58]

With the balanced resection technique, the tibial cut is performed first and after this, symmetrical tension is applied to the extended joint using a ligament tensor, knee balancer or spreaders. This should show any extent of varus/valgus deformity, which should be corrected by ligament balancing. The same process is then used in 90° flexion, where the joint is distracted. The femoral component is then set using ligament tension rather than anatomical landmarks. [57]

Both presented techniques try to correct allignment first. Usually 61–88 % of balanced knees meet the required 0–3° tolerance. Afterwards they try to achieve an equal flexion/extension gap with a gap difference lower than 1 mm. In 84–90 % knees a balanced rectangular gap is present. [54, 57]

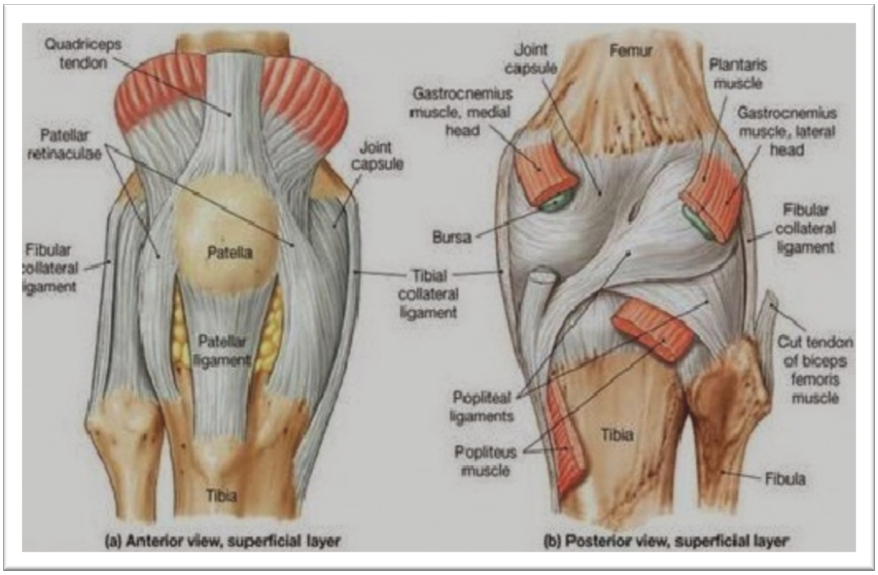

Figure 15: Superficial layer of Knee ligaments [62]

2.7.2 Valgus knee

A valgus knee presents with two major characteristics – it has higher bone damage of the lateral condyle and tighter lateral ligaments. They include the lateral collateral ligament, iliotibial band, popliteus tendon and posterolateral capsule. Over the time, several techniques have been described for balancing this deformity. [61]

Whiteside pointed out, that the popliteus tendon, LCL and posterolateral corner of the fibrous capsule influence both flexion/extension. The LCL and capsule impact the extension more, while the popliteus tendon is more effective in extension. According to his method, the knee should first be balanced in flexion, with the initial release of the popliteus tendon, followed by the lateral collateral ligament and lastly the fibrous capsule. If there is any leftover tension in extension, the iliotibial band can also be released. [55, 57, 58]

Another method was presented by Favorito. In his work, the tightest lateral structure, which most frequently is the LCL, should be released first. This should be followed by the release of the popliteal tendon, capsule and if necessary, the gastrocnemius muscle can be released as well. To remove any further tightness, the iliotibial band can be resected, while

the popliteal tendon and LCL can be sutured together to provide further flexion stability. [57]

If the valgus deformity is lower than 20° (figure 16), the pie-crust technique can be used. It includes several horizontal incisions, with the depth being lower than 5 mm, along any tight lateral structures. [57, 58]

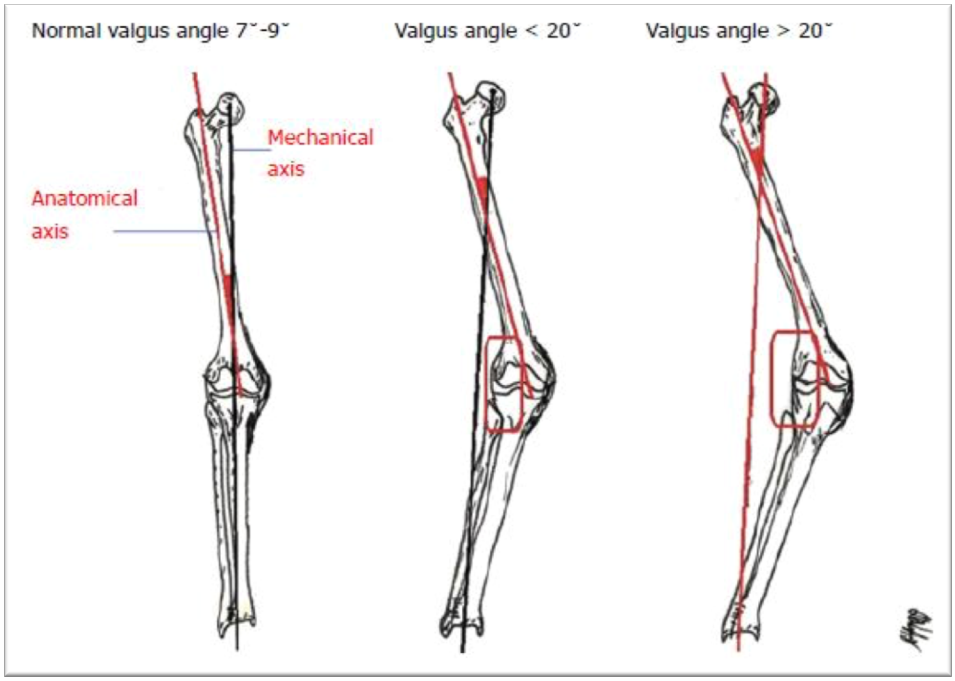

Figure 16: Different stages of valgus knees [63]

On the other hand, deformities greater than 15° in severe valgus knees can be corrected using a cruciform lateral approach. A laminar spreader is first introduced to rotate the femoral component, which should ensure a symmetrical gap in flexion. Afterwards the tibial cut is performed in addition to extension balancing. The cruciform approach is connected to two cuts – the first one vertically in the retinaculum and the second one at the joint line and 1–2 cm anteriorly/posteriorly. [57, 58]

Lombardi's method starts with the iliotibial band release. The posterolateral capsule is released from the distal part of the femur. If further balancing is required, the popliteal tendon and LCL can also be released. [57]

Ranawat introduced an inside-out technique which can be used for severe valgus knees as well. The process is very similar to all the above presented techniques, but puts more importance to the PCL release and recommends the use of electrocautery in the release of the capsule. [57]

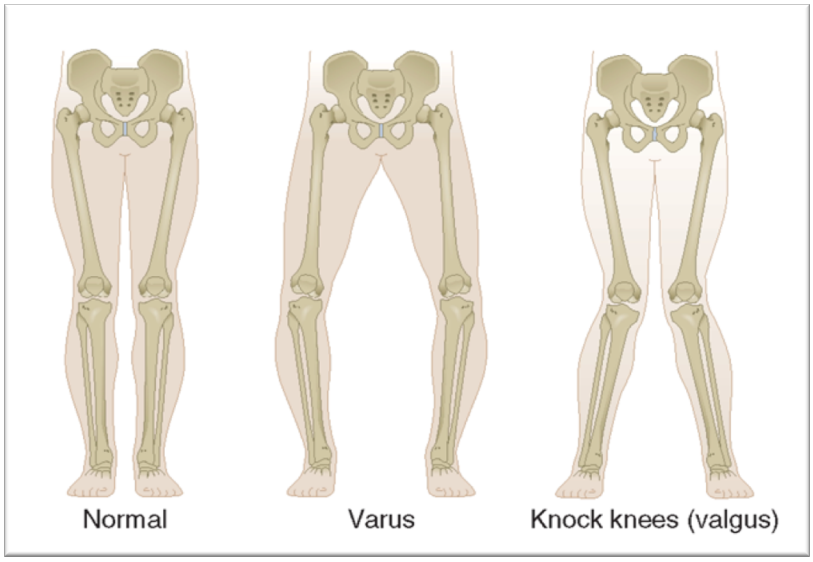

Figure 17: Comparison of a Normal, Varus and Valgus Knee [64]

2.7.3 Varus knee

Varus knee (figure 17) is considered the easier one to correct. In small deformities, removing osteophytes might be enough to balance the knee sufficiently. The semimembranosus tendon is released and the medial collateral ligament might be released as well, if the knee is still too tight in extension. Burke recommends releasing the MCL subperiosteally first, followed by the superficial release. Further medial structures can be released to provide more balance if necessary (pes anserine, posterior capsule, medial m. gastrocnemius). (17, 58]

Whiteside's theory for knees tight in flexion advocates releasing the anterior part of the MCL first, with the posterior part being released only when the knee is tight in extension. [57]

2.7.4 Posterior Cruciate Ligament

The PCL's role in ligament balancing can also contribute to proper stabilisation. In 20 % of all TKR, the PCL is divided to achieve a balanced flexion gap. The correct function and tension of the PCL is especially important when using a cruciate-retaining prosthesis. The PCL might be resected if necessary, for better flexion and to minimize the risk of possible PCL damage. [60]

2.8 Wear tribology

Tribology describes the intraction of surfaces during their movement. It includes the study in fields of friction, wear and lubrication. Friction can be desired, but also unwanted in many situations of everyday life. The goal in joint replacements is to minimize friction and wear, because these properties highly influence the lifetime of implants. The wear of implants is still one of the most common reasons behind implant failures. Particles that are released in the proces of friction and wear can also contribute to the occurence of infection. Therefore, the study of wear in joint implants is highly important.

The two most frequent types of friction are dry and lubricated friction, which is when a fluid lubricant separates two solid surfaces. Lubricated friction and its‘ phases are described by Stribecks‘ curve. It describes the fluid-lubricated friction as a non-linear function of the contact load, the lubricant viscosity and the lubricant entrainment speed. This relationship is characterized by Hersey’s number, defined in the following relationship, where μ is the dynamic viscosity of the fluid, N its entrainment speed and P is the normal load. [65]

$$Hersey\ number = \frac{\mu * N}{P}$$

The Stribeck curve (figure 18) is divided into four lubrication regimes. [66]

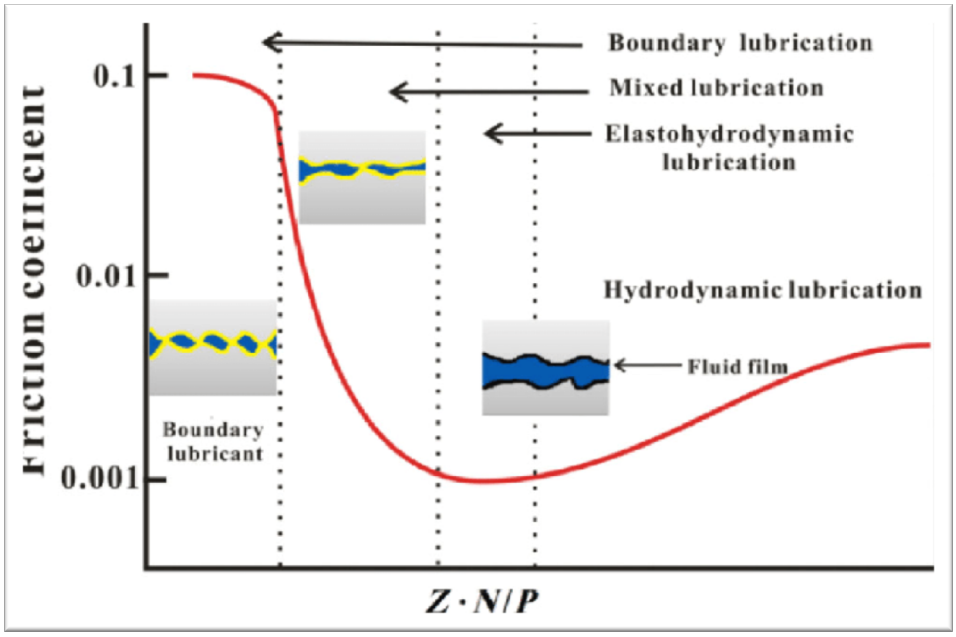

Figure 18: Stribeck curve [67]

1. Boundary lubrication occurs when the two surfaces come into contact. The load is supported mainly by surface asperities. The friction during this period is very high. [65]
2. Mixed lubrication means that the load is supported by the mix of surface asperities as well as the liquid lubricant. [65]
3. Elastohydrodynamic lubrication happens when elastic strain occurs at the contact interface. The motion of the two contacting surfaces creates a flow that induces pressure, which then supports load. Asperities are sparse. [66]
4. Hydrodynamic lubrication means that almost no asperities occur, and the load is supported mainly by hydrodynamic pressure. [65]

The roughness of joint cartillage is usually 0.07–0.45 μm, during local loading this value lowers to just 0.01–0.03 μm. The friction coefficient is 0.05–0.037. In comparison the friction coefficient between CoCrMo x CoCrMo implant surfaces is 0.25 and between CoCrMo and UHMWPE 0.07. The improtance of lubrication fluid is therefore very important and its insufficient amount leads to higher and undesired wear.

Practical Part

In the practical part of my diploma thesis I am going to analyse the linear wear of a balanced and unbalanced knee implant. I will first present a FE (finite element) model of the knee implant with loading and displacement based on ISO 14243-3 and then a standard wear test, which used the same loading and displacement parameters as the FE model. Both of these will be done in a balanced and unbalanced state. [68]

3.1 Loading and displacement

The FE model and the wear test were loaded according to the international standard ISO 14243-3, with small alterations. This standard prescribes the principle and load/displacement functions of the implant during a standardized wear test. [68]

3.1.1 Reference position and axes definition

The reference position describes the state, where the tibial component pushes against the femoral head with a positive axial force and the tibial component is in static equilibrium.

The tibial axis corresponds to the longitudinal central axis of the proximal tibia (position 2 in figure 19). The axial force axis is then defined as a translation of the tibial axis in the medial direction by $0.07\,w \pm 0.01\,w$, where w is the width of the tibial component. The flexion/extension axis is defined by a zero flexion angle, when the tibial component is in static equilibrium. [68]

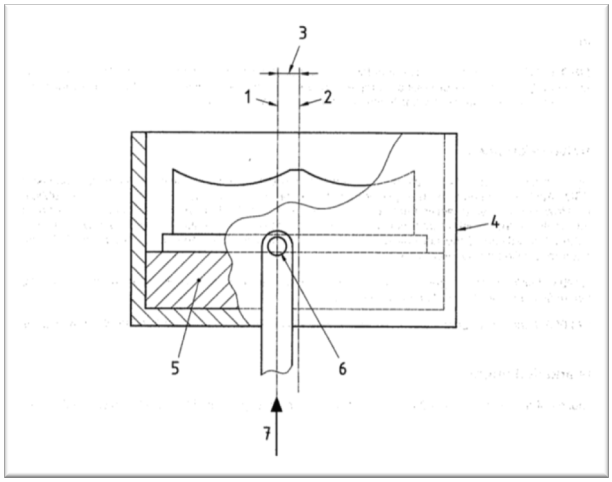

Figure 19: Visualisation of the tibial insert inside the simulator [68]

3.1.2 Axial force

An axial force (figure 20) is applied by the tibial component on the femoral component and the direction is parallel to the tibial axis. The positive sense of loading is prescribed in the inferior-superior direction. [68] The axial force was adapted slightly, and it stays at 630 N after 60 % of the cycle to eliminate impacts between the tibial and femoral component.

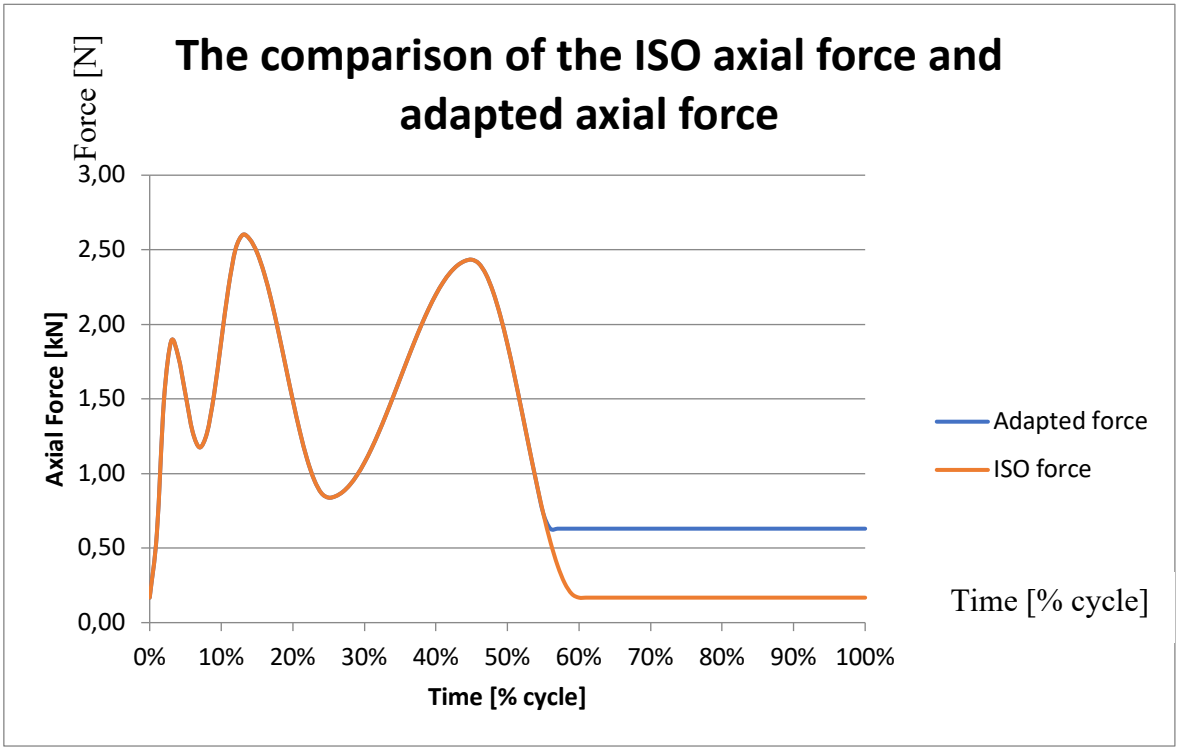

Figure 20: The comparison between the ISO axial force (orange) and the adapted axial force (blue) [68]

3.1.3 Flexion/Extension

The knee flexion and extension is defined around a rotational axis, which is not exactly the same as in the human body, but should be withing reason according to the possibilities of the laboratoral environment. The positive sense corresponds to the posterior motion of the femoral component. [68]

3.1.4 Anterior/Posterior displacement

The anterior/posterior displacement equals the offset between the femoral and tibial component in a direction that is perpendicular to the force and flexion/extension axes. The positive sense is defined as the anterior movement of the tibia to its' reference position. [68]

3.1.5 Internal/external rotation

The intenal/external rotation equals the rotation of the tibial component around its‘ axial axis. The positive sense is described as a clockwise movement when looking at the tibial component from a superior position for a left knee. [68]

3.1.6 Cycle duration and parameters

The simulator operated at a frequency of 0.5 Hz, meaning that one cycle lasted two seconds. The end of the wear test was set to 500 000 cycles. The temperature was held at 37 $\pm$ 2 $°C$ and the wear simulation was lubricated (further described in chapter 3.3.4).

3.2 FE Model

I developed a FE model of the knee implant (figure 21) using the commercial Pam Computational Environment during an internship at Mecas Esi s.r.o. to evaluate the stress distribution and average contact pressures on the tibial insert of a balanced and unbalanced knee implant.

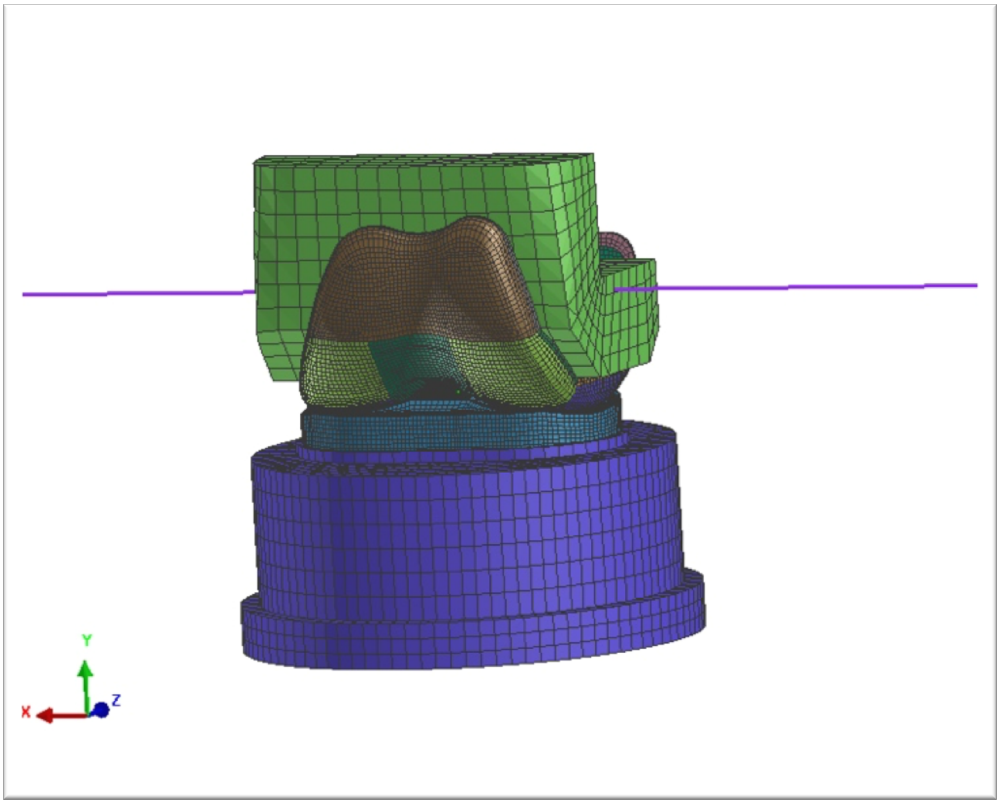

Figure 21: FE model of the knee implant and its holders

3.2.1 Model Setup

During the wear test, the tibial insert and femoral component are attached to a special set of holders, which were created and designed specifically for the attachment during knee wear simulation. The rotation axis of the femoral component was created geometrically.

3.2.1.1 Mesh

The tibial insert and femoral component were imported directly from a CAD model, while the holders were simplified and modelled according to their drawings. All components were messhed using the Hypermesh software with approximately 1 mm hexahedral and tetrahedral elements for the UHMWPE insert and femoral component, whereas 3 mm hexa/tetrahedral elements where used for the holders, since they will not be directly evaluated. The mesh was also locally refined, where needed, to eliminate any hard lines. These mesh values were based upon literature research and personal experience and were also compared to two coarser mesh sizes, which used 2.5 mm (mesh 1, figure 22) nad 1.5 mm (mesh 2) hexa/tetrahedral elements for the tibial insert, to ensure the selection of the mesh size does not affect the results. [69, 70]

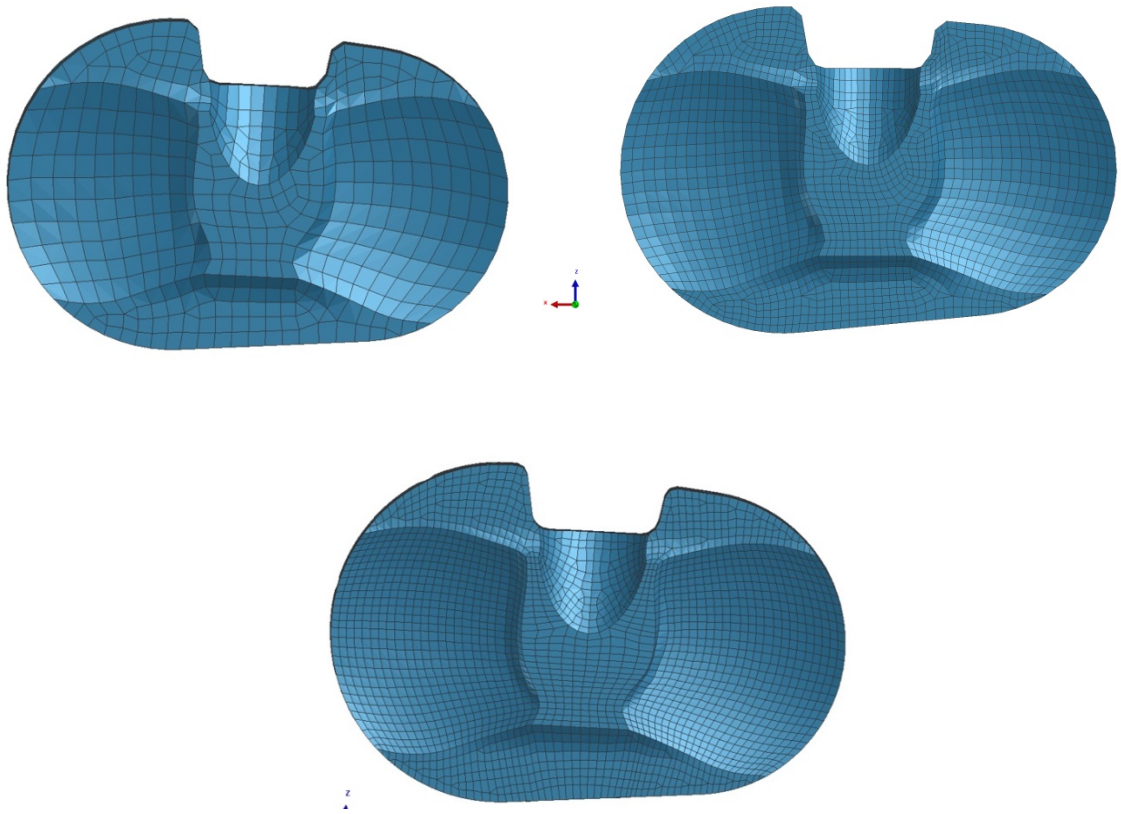

Figure 22: Comparison of three different element sizes. The picture on the top left shows the coarser mesh with 2.5 mm elements, the top right shows the 1.5 mm mesh and the final 1 mm mesh can be seen on the bottom.

A simplified model was used for the mesh comparison. The model was only loaded with a 2.6 kN axial force, which corresponds to the maximal value of the axial loading curve in the ISO standard. The boundary conditions were set to 111111(translation in x, y, z and rotation around x, y, z respectively) for the femoral component/holder and 100100 for the tibial component/holder.

Table 1: The comparison of three selected mesh sizes

Mesh	Number of elements	Tibial insert stress maximum (MPa)
Mesh 1 (2.5 mm)	13879	24.29
Mesh 2 (1.5 mm)	26375	25.97
Mesh 3 (1 mm)	59105	26.49

The maximal von Mises stress values in the tibial insert for the three compared mesh sizes are presented in Table 1 and visualized in Graph 1. The maximal stress values converge to the value of the 1 mm mesh, which was selected for the experiment.

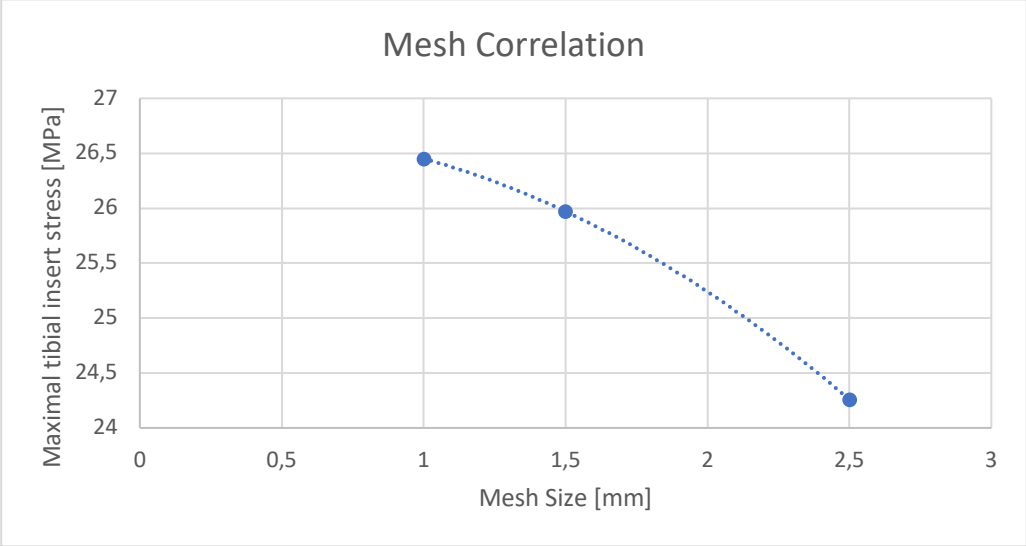

Graph 1: The comparison of the three selected mesh sizes and their maximal stress values

3.2.1.2 Materials

The materials used for each part are described in table 2. The material used for the holders was steel 1.4301. The femoral component material was CoCrMo and the tibial insert material was UHMWPE. All three materials were considered to be elastic solids. [71, 72, 73]

Table 2: Materials used in the FE model

Part	Material	Type	E (GPa)	Poisson‘s ratio (-)
Holders [71]	Steel 1.4301	Elastic Solid	200	0.28
Femoral component [72]	CoCrMo	Elastic Solid	210	0.29
PE insert [73]	UHMWPE	Elastic Solid	1.1	0.42

3.2.1.3 Contacts and Boundary Conditions

The contact between the UHMWPE insert and its‘ holder, as well as the contact between the UHMWPE insert and femoral implant was modelled using a Node-to-Segment contact with edge treatment. A tied link was also created between the femoral implant and its‘ holder. Boundary conditions were set up for the UHMWPE insert holder as 100100 and for the femoral component a 111011 boundary condition was applied. A multiple constraint was used to tie together the rotation of the femoral component around the rotational axis. The tibial insert holder was set up as a rigid body.

3.2.1.4 Forces and Loading

The flexion/extension and internal/external rotation were simulated using angular rotation, the anterior/posterior movement of the tibial part using a displacement function and the axial force using a concentrated load function. All of these functions were set up according to chapter 3.1.

Two versions were created. One corresponding to the conditions described above and the second version included two additional forces of 132 N on the bottom of the UHMWPE insert holder (figure 23) acting in the opposite direction. One acted in the center of the tibial insert holder and the second acted at a moment arm of 41 mm to create an additional torque

on the medial condyle. These values were based on the spring selection in the wear experiment (will be explained in chapter 3.3.6).

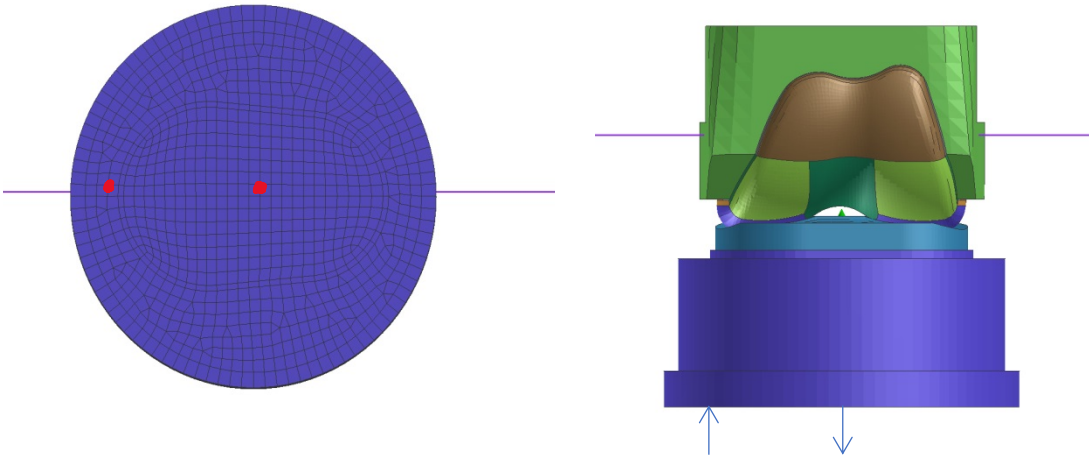

Figure 23: The position of the two added forces is shown on the left picture and marked by the red dots. The sense of the two forces can be seen on the right picture.

3.2.2 Evaluation

The models were evaluated in the Visual Viewer software, where maps of von Mises stress distribution were obtained. Based on the distribution of von Mises stress, three nodes were selected on each condyle (N1-N6, figure 24 as well as one reference node (R). The average contact pressures in these seven selected nodes were aquired for the balanced and unbalanced model and compared. Using the six condylar nodes, the percentual change in contact pressure between the balanced and unbalanced model for both medial and lateral condyle was evaluated.

To compare the results of the FE model and the actual wear test, I used the Archard model equation. It describes the linear wear depth W_n, where k_A is Archards constant of adhesive wear ($7.64*10^{-10}$ m^2/N in this case), P is the average nodal contact pressure and S is the nodal sliding distance magnitude. [74]

$$W_n = k_A * P * S$$

I calculated the wear depth for the seven selected nodes in the balanced and unbalanced state and compared them.

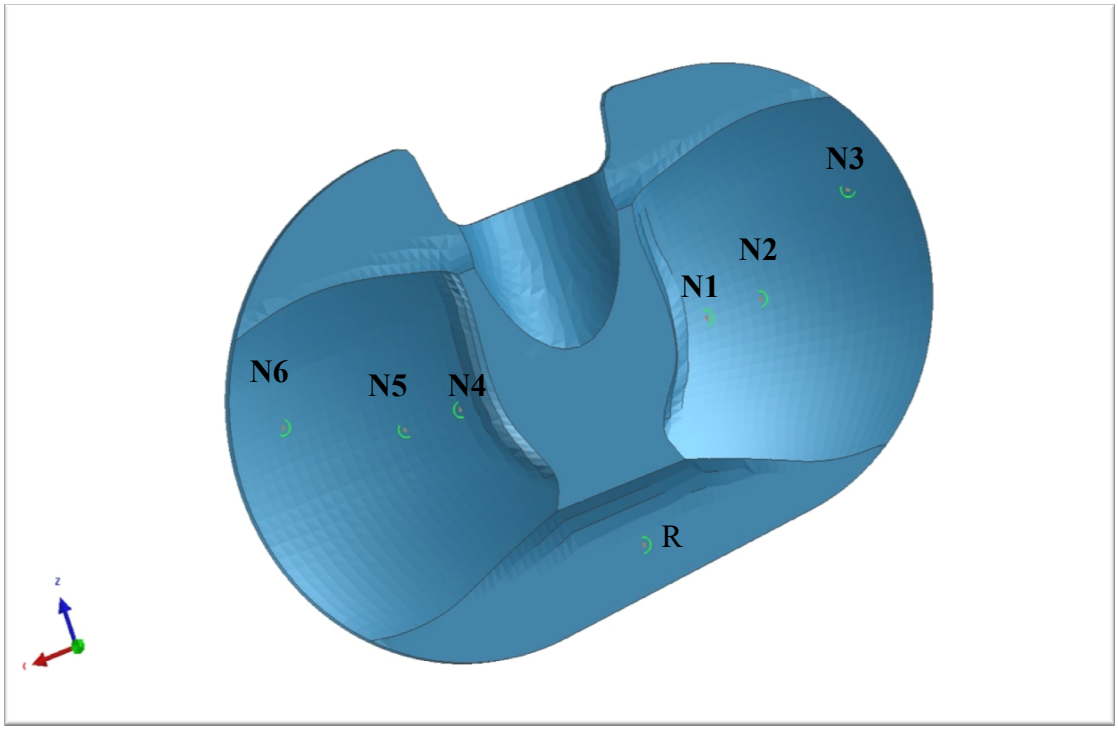

Figure 24: The location of evaluated nodes

3.3 Wear Test

To evaluate the wear of a balanced and unbalanced knee implant, two UHMWPE tibial insert samples were tested according to chapter 3.1. Each sample underwent the same experimental steps:

1. Surface scanning before the wear test
2. Wear test
3. Surface scanning after the wear test
4. Evaluation of the two scans using CloudCompare software

3.3.1 Tibial implant samples

Two tibial insert samples were provided by the company Beznoska s. r. o., which manufactures implants, tools and surgical utensils for orthopedic and traumatological purposes. Both samples were 4th generation virgin cross-linked UHMWPE left knee tibial inserts (type SVL, figure 25).

Figure 25: Tibial insert type SVL [75]

3.3.2 Surface scanning

The surface scanning of both samples was done using the optical 3D coordinate measuring system RedLux Ltd. This device (figure 26) scans the sample using a contactless probe and reconstructs the geometry with high definition and therefore allows us to analyse the wear of a sample.

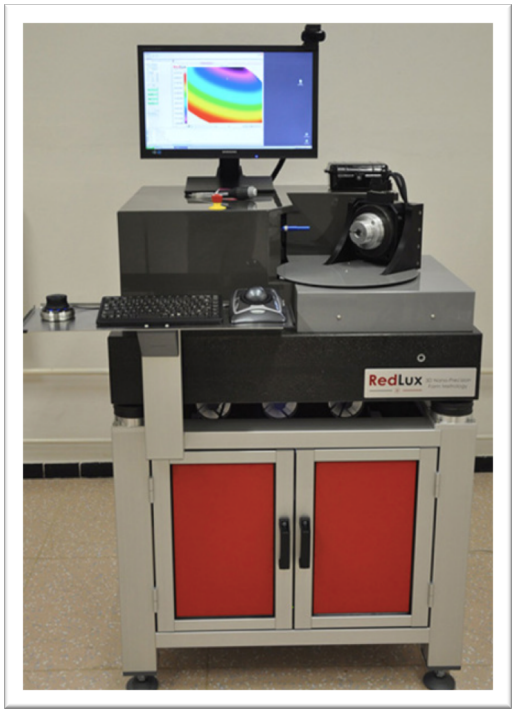

Figure 26 : RedLux scanning system [76]

This measuring system consists of two linear and two rotational axes. The scanned subject is moved using the rotational motors, while the probe moves within the linear axes. Parameters of the RedLux scanner can be observed in table 3

Table 3: RedLux measuring system parameters [75]

Measuring range	300 μm
Working distance	4.5 mm
Definition in the Z coordinate	10 nm
Probe diameter	15 mm
Overall device precision for general surfaces	2 μm + 0.1 μm * L/mm

3.3.3 Simulator KKK ELO

Two wear tests were conducted using the KKK ELO simulator (figure 27), which was specifically designed for realistical simulations of wear tribology of human joints. It can simulate flexion/extension, anterior/posterior movement and internal/external rotation and therefore can be used for wear tests according to the ISO 14243 standard. [68]

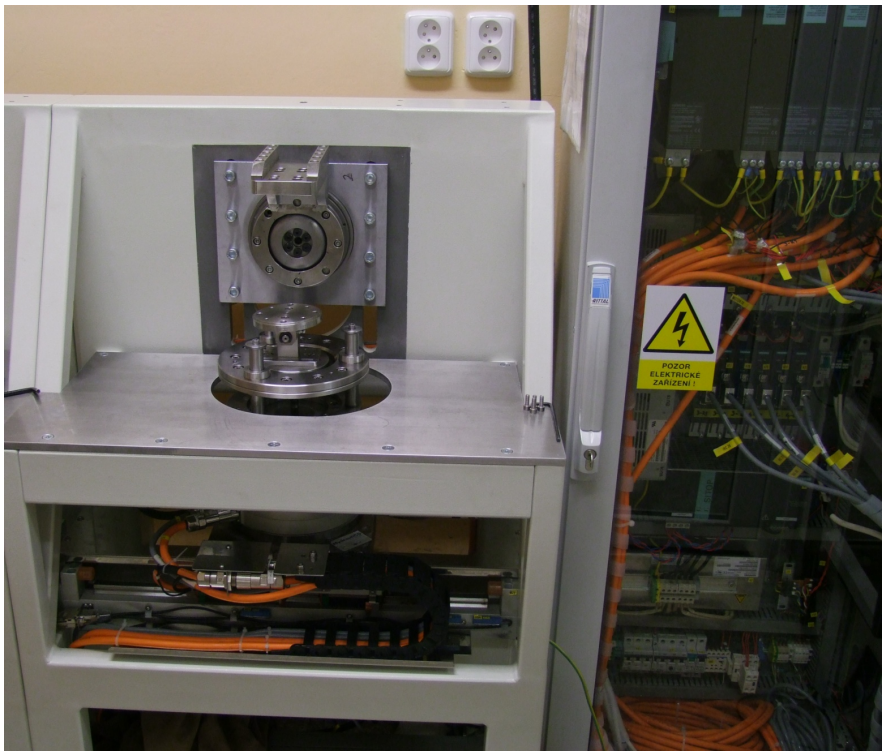

Figure 27: KKK ELO 2011 Simulator

The linear motor is responsible for the anterior/posterior movement, while two rotational motors create the flexion/extension as well as internal/external rotation. The rotational motor includes an air cylinder, which creates an axial force that acts on the tibial component in a distal-proximal direction. This force presses the tibial component against the femoral head according to the used standard (figure 28).

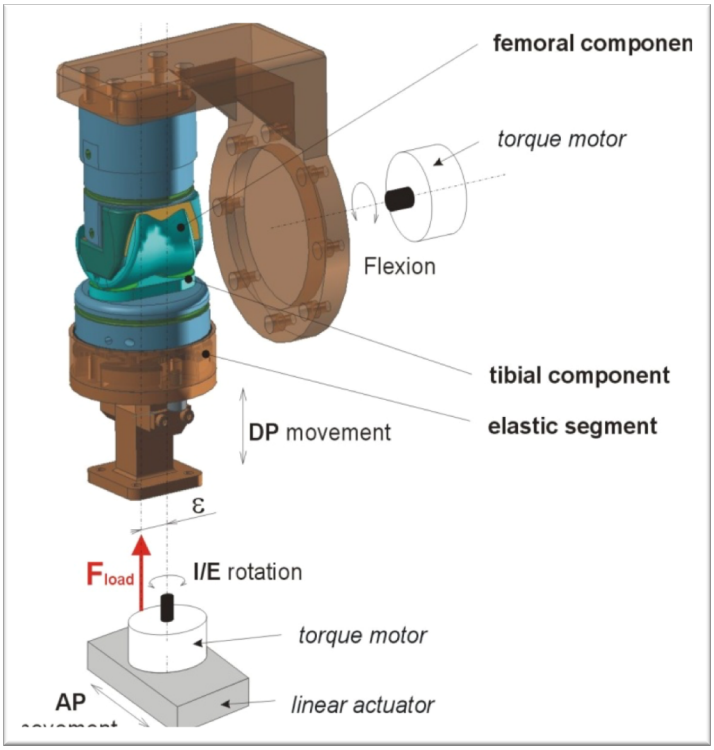

Figure 28: Setup of the KKK ELO simulator for knee wear simulations [77]

Some of the parameters and ranges of the KKK ELO simulator can be observed in Table 4.

Table 4: Range of motions of the KKK ELO 2011 simulator [77]

Motion	Motor	Range
Flexion/extension, internal/external rotation	Torque motors	0–360 degrees
Anterior/posterior movement	Linear motor	± 40 mm
Distal/proximal movement	Hydraulic system	± 40 mm

3.3.4 Testing Lubricant

The testing lubricant serum was prepared according to ISO 14243 [68]. It countains bovine serum mixed with distilled water. In order to slow down the degradation of this mixture penicilin and disodium were added. The pH and volume of this lubricant can

be controlled by the simulator. The following (table 5) quantities were used to achieve the desired ratio of the components. There is no specific volume defined by the standard, but the contact surfaces must be immersed in the fluid at all times, which in my case meant adding around 50ml of lubricant.

Table 5: Testing serum composition

Bovine serum	0.5 l
Distilled water	1.1 l
Penicilin	15 ml
Disodium	9.7 g

3.3.5 Experiment setup

Two wear simulations were conducted (figure 29) based on ISO 14232 [68] with small alterations as described in chapter 3.1. The operating frequency was $0.5\,Hz$ (instead of 1 Hz) and the axial force function stayed at 630 N after 60 % of the cycle time. The samples were heated to $37 \pm 2°C$ according to the standard to reflect the human environment. The simulation ran 500 000 cycles due to time purposes and higher loading.

Figure 29: Experiment setup

The samples were attached to special holders (stainless steel 1.4301), which were designed for knee wear simulations. The femoral component was made from CoCrMo. After both femoral and tibial components were attached to the holders, a latex poutch was pulled over them. The inside of this poutch was covered with sanitary silicone to prevent latex particles from infiltrating the lubricant during the testing. The lubricant was introduced after this.

Both tibial insert samples were tested using this basic setup, but one of the simulations included an added rotational torque, which was created by adding an extra spring to the experiment setup. This simulated the unbalanced state of the knee implant.

3.3.6 Spring Selection

An additional spring was added to the experiment (figure 30) to simulate the unbalanced state of the knee implant by enhancing the knee torque on the medial side to reflect a varus deformity, which is more frequent than valgus.

Figure 30:The position of the spring in the simulator

The imbalance of the knee joint is usually only described by the gap difference between the femur and tibia since there is no direct force or torque measure, which could quantify the imbalance of the ligaments. Therefore, it was difficult to put a specific number on the actual force to be used for the spring selection. I conducted a literature search and compared the contact forces between balanced and unbalanced knees as they were presented in these selected papers. These forces were usually taken from graphs showing the force distribution on the tibial insert, which do not correspond to the actual position of the spring. The difference between the balanced and unbalanced knee forces had to be recalculated to represent the actual position of the spring in the wear simulation and to achieve a similar additional torque. These forces also represented different body weights, severities of the varus deformity and loading conditions. Therefore, they were used more as a guideline as to how big these forces and resulting torques could be. For example, sources 78, 79 and 80 only considered the body weight force, while source 81 considered a 4000 N load at the hip joint, so I recalculated the values proportionally to reflect loading of the knee joint by the body weight of a 75 kg person. These forces also acted at a certain distance from the center of the tibial insert, while the selected spring for the experiment would have a definite moment arm of 41 mm, so I recalculated the torque these forces would cause for this moment arm (table 6).

Table 6: Forces used for the calculation of the spring force [78, 79, 80, 81]

Medial Compartment Force (N)		**Recalculated Force difference (N)**	**Recalculated Torque (N/m)**	**Source Citation**
Normal	**Varus**			
160,5	201	80	3.2	78
155.25	172.5	72	2.88	79
95	185	100	4	80
944	1047	206	8.24	81

Based on this information, I was looking for a commercially available spring that would provide a torque of roughly 5–6 N/m at a 41 mm moment arm and would fit into the simulator peg, which had a length of 43 mm and an outter diameter of 10.1 mm. According to this, I selected a spring from the company Hennlich with a force of 132.1 N when fully

compressed, which will result in a additional torque of 5.2 N/m. The parameters of the spring are described in the following figure 31 and table 7.

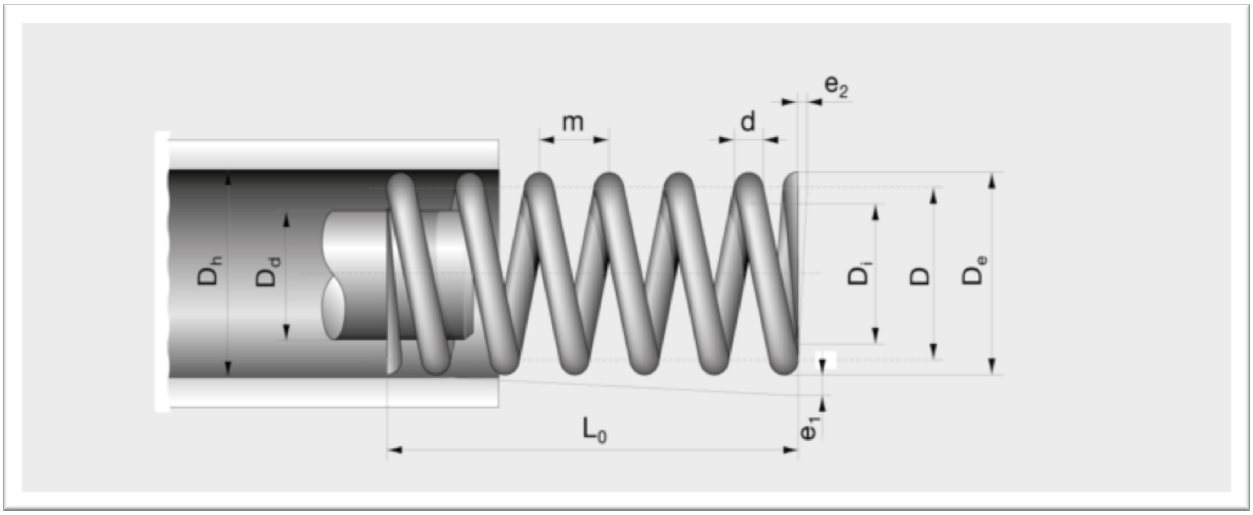

Figure 31: Description of spring parameters [82]

Table 7: Parameters of the selected and used spring [82]

d	1.6 mm
D_e	14.1 mm
L_0	115 mm
L_n	42.2 mm
Material	1.1200
Force	132.1 N

3.3.7 Evaluation

Each tibial insert was scanned using the RedLux measuring system before the experiment and after 500 000 cycles, therefore 2 scans were obtained of each sample. These scans were evaluated using the CloudCompare software. Cloudcompare is a free 3D point cloud processing software which provides tools for rendering and meshing. It offers advanced processing algorithms for example for projections, distance computations or geometric features estimations. Every scan consists of a large number of points described by their xyz coordinates. The initial scan of the balanced insert had 93 437 points and 143 784 points after the experiment. The initial unbalanced insert scan had 105 835 points and 60 983 points after 500 000 cycles.

For each simulation (balanced/unbalanced), both the before and after 500 000 cycles scans were imported. The before scan was meshed using the best fitting plane function (figure 36). Before the two scans could be alligned, the points with the highest wear were hidden, so that they don't affect the allignment process. Then both scans were manually alligned, after which a rough fit was computed by selecting 4 equivalent point pairs. After that, a fine fit can be computed. The initial root mean square (RMS) difference was set to $1e^{-50}$ and the random sampling limit to 150000 to involve all possible points.

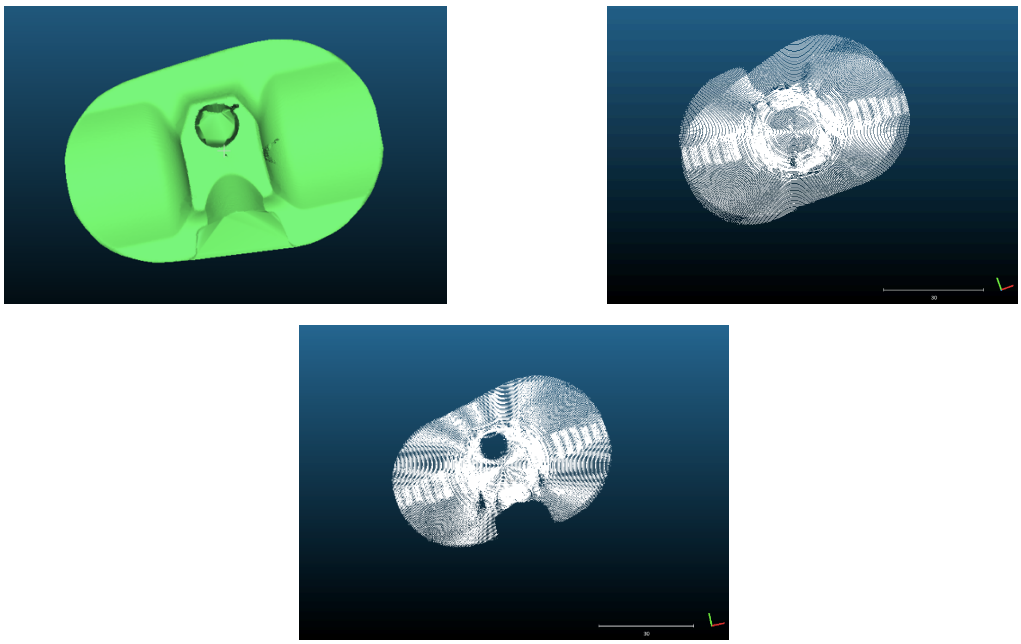

Figure 32: Meshed point cloud (left), the two unalligned imported point clouds (right), point clouds after initial rough allignment (bottom)

Once the two scans were alligned, a cloud to mesh distance function could be used to analyze the surface changes between the two tibial inserts. CloudCompare first calculates approximate distances, which are used to select the best octree (tree data structure, each internal node has 8 children nodes) level for the actual distance computation. This computation can then be helpfull when selecting the actual maximum distance for computation, since large distances lead to very long computation times.

Results

4.1 FE Model

The results of the FE model simulation show comparable von Mises stress values and distribution in both balanced and unbalanced state of the polyethylene insert. The maximal von Mises stress in the unbalanced state was 41.99 MPa (figure 34), whereas for the balanced simulation it was only 39.50 MPa (figure 33). Both maximal states occured at the same time (14 % of the cycle). The unbalanced state did not lead to a dramatic increase in the maximal value, since the change is only 2.49 MPa (6.3 %).

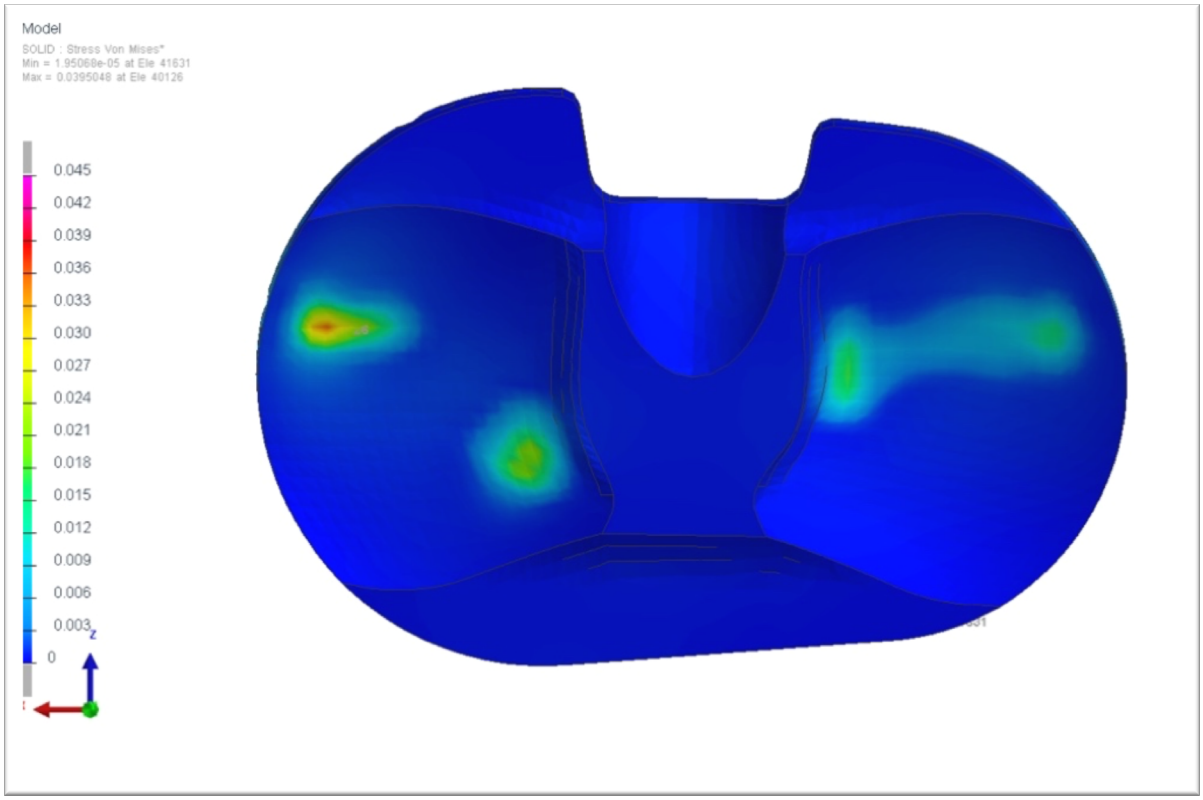

Figure 33: Maximal von Mises stress value (39.50 MPa) and distribution in the normal simulation. The distribution is described by the scale on the left side, with tha maximal values being red and minimal values being blue.

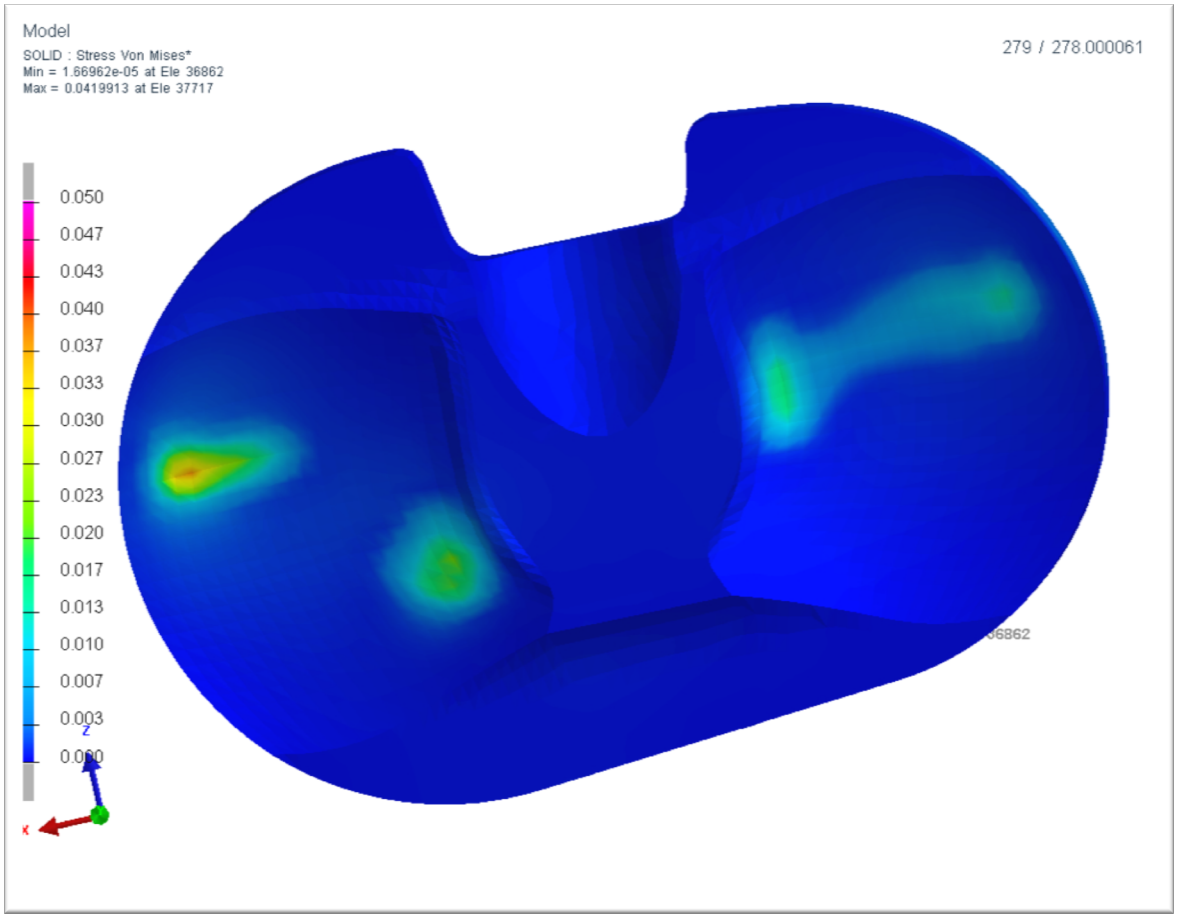

Figure 34: Maximal von Mises stress value (41.99 MPa) and distribution in the unbalanced simulation. The change as compared to the balanced state in Fig. 33 is minimal. The color scale is described on the left.

The average contact pressure values for the seven selected nodes (table 8) in the balanced and unbalanced model show an increase in average contact pressure for two nodes on the medial condyle, where the extra force was added.

Table 8: Total contact pressure values during one simulation cycle for the selected nodes in the balanced and unbalanced simulation.

Condyle	Node	Normal [MPa]	Unbalanced [MPa]	Difference [%]	Condyle pressure difference [%]
Lateral	N1	15.85	15.36	-3.09	-5.78
	N2	1.11	0.52	-53.15	
	N3	5.68	5.45	-3.54	
Medial	N4	10.26	9.62	-6.23	+16.49
	N5	1.82	3.67	+101.64	
	N6	8.71	10.93	+25.48	
Reference	R	0	0	0	-

The highest average contact pressure on the lateral condyle was in node 1 for both simulations - 15.85 MPa for the balanced state and 15.36 MPa for the unbalanced state (decrease by 3.09 %). On the medial condyle, the highest average contact pressure for the unbalanced simulation was 10.93 MPa in node 6, which meant an increase by 25.48 % from the balanced model (8.71 MPa). The average contact pressure on the lateral condyle decreased by 5.78 % in the unbalanced model (as compared to the balanced model), while an increase of 16.49 % was present on the medial condyle. The percentual change of average contact pressure for the selected nodes (figure 35) describes the increase in average contact pressure in the unbalanced medial condyle.

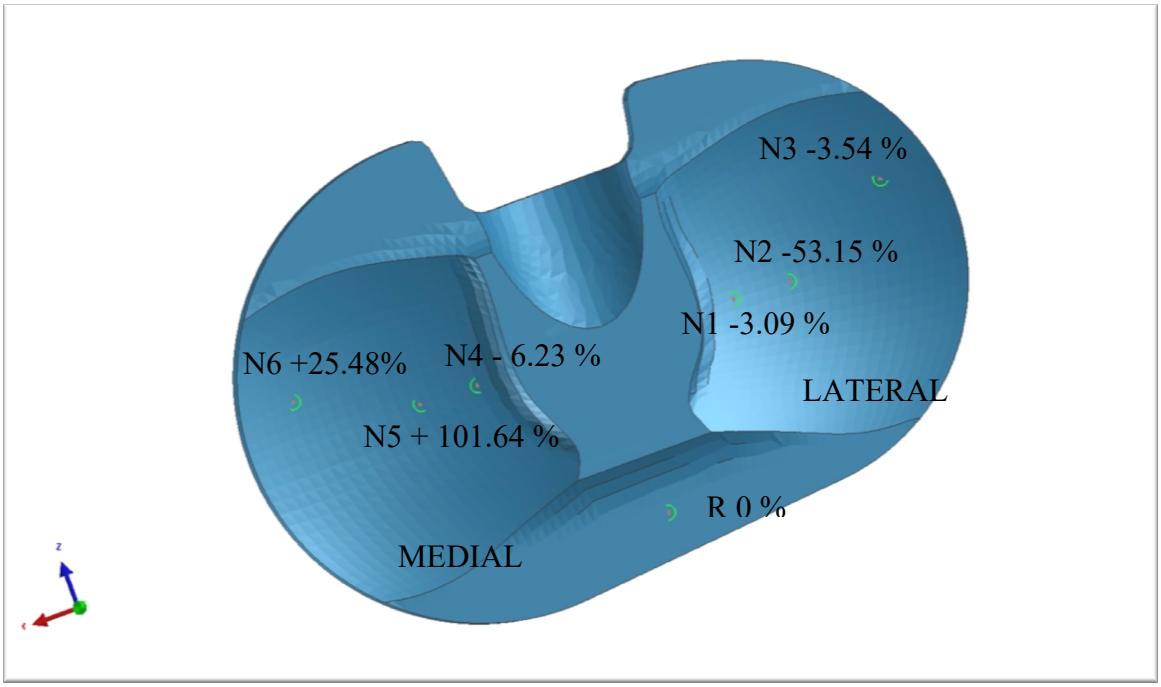

Figure 35: The percentual change in average contact pressure between the balanced and unbalanced state for the selected nodes N1-N6.

The linear wear depth was evaluated according to Archards equation for 500 000 simulation cycles (table 9). The unbalanced model showed an increase in wear depth on the medial condyle for nodes 5 and 6. For node 5 the increase was 109.10 % and the unbalanced wear depth 0.046 mm, for node 6 the increase was 40.54 % and the unbalanced wear depth 0.156 mm, which was the maximal calculated wear depth on the medial condyle. The lateral condyle presented with lower wear values in all three nodes, with the maximal change of -46.15 % in node 2, which was positioned in the center of the lateral condyle. The highest wear depth noted on the lateral condyle was 0.197 mm in node 1.

Table 9: Estimated linear wear depth according to Archards law based on the values received from the FE model and calculated for 500000 simulation cycles

Node	Balanced Model Wear Depth [mm]	Unbalanced Model Wear Depth [mm]	Difference [%]
N1	0.204	0.197	-3.43
N2	0.013	0.007	-46.15
N3	0.081	0.077	-4.94
N4	0.124	0.116	-6.45
N5	0.022	0.046	+109.10
N6	0.111	0.156	+40.54
R	0.000	0.000	0.00

4.2 Wear Experiment

The linear wear evaluation of the tibial articulating surface after 500 000 cycles during the standard knee wear experiment (figure 36) shows an even wear distribution on both condyles. The values are described by the color scale on the right side, with red symbolizing areas with maximal wear and blue/green areas with zero linear wear. The maximal wear values are located in the central areas of the articulating condyles and reach 0.12 mm. The wear areas around the central hole were caused by the simulator rather than the experiment, therefore they should not be considered.

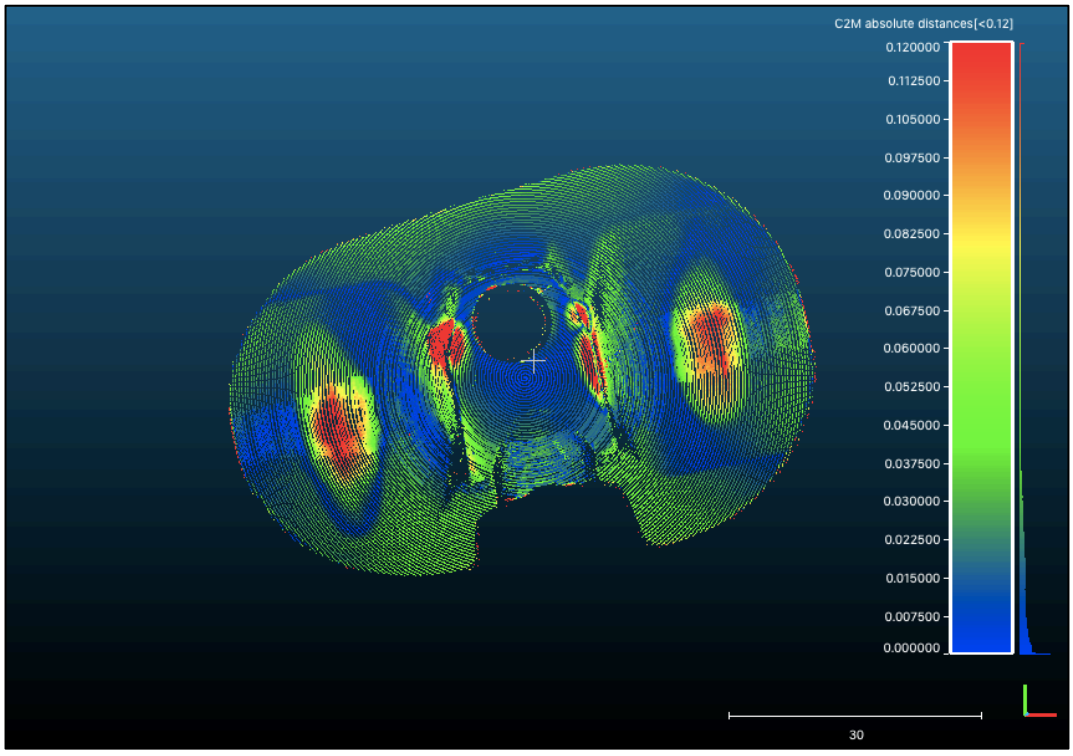

Figure 36: Evaluation of linear wear of the balanced tibial insert after 500 000 cycles

The evaluation of the tibial insert scan after 500 000 cycles in the unbalanced state, evoked by the added spring torque, (figure 37) shows a slightly different wear pattern than the balanced insert. The higher linear wear values are slightly shifted to the medial condyle and its maximal values are also around 0.12 mm. The wear on the unbalanced medial condyle is more centered in one location, whereas on the left condyle the wear path is elongated along the whole contact area. Overall, there aren't any conclusive differences between the balanced and unbalanced scan evaluations, since the changes in both linear wear values and distribution are minimal.

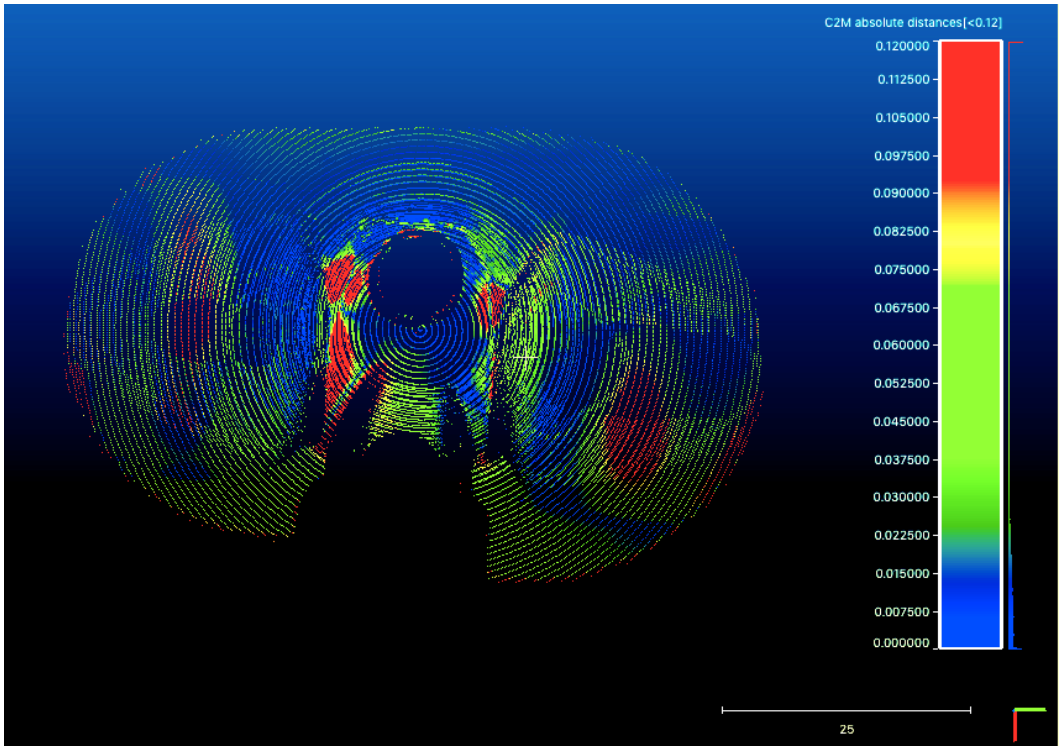

Figure 37: Evaluation of linear wear of the unbalanced tibial insert after 500 000 cycles

Discussion

The results of the FE model evaluation in the balanced state are consistent to previously done experiments, where maximal von Mises stress values ranged from 35-37.5 MPa and contact pressure values were also comparable [74, 82, 83]. I could not find a similar FE analysis of the unbalanced knee implant using an added spring to simulate the additional torque. Other authors tilted the tibial component by various angles (usually 5°) to simulate varus/valgus malalignment and they achieved an increase in von Mises pressure by 2.4-10 MPa [84,85], although this is also comparable to my results in the unbalanced state. None of the authors used the FE model to predict linear wear according to Archard equation in relation to incorrect ligament balancing. Also, there has not been done a similar wear experiment to investigate the effect of ligament balancing on implant wear and lifetime, so these results cannot be compared to other authors. However, authors that did study the effect of malalignment of the knee implant did conclude, based on their mentioned results, that proper alignment is crucial for a functional knee replacement and poor alignment can lead to ligament laxity and shorter implant lifetime [83,84].

My study did show comprabale results between the FE model and wear experiment. The FE model showed higher differences between the balanced and unbalanced state in all discussed parameters– von Mises stress, average contact pressure and linear wear, while the change in linear wear in the tibial insert scans was minimal. This could be due to the experiment setup, where a spring was used to simulate the unbalanced state. Since no previous study has tried to simulate the unbalanced state of the knee implant, this approach was based on personal understanding of the issue and research. The tibial holder in which the spring was placed, was stiffer due to issues with the simulator, meaning that the created torque by the spring was probably smaller. The evaluation from the FE model was also based on just seven selected nodes. Since the numerical increase of the discussed parameters in the FE model wasn't that significant and the wear experiment did not show any major changes in linear wear of the tibial insert, I would not conclude, based on my results, that improper ligament balancing causes sooner implant failure.

Based on my current knowledge after the experiment, I would test several possible forces in the FE model, to see how these imbalances affect the von Mises stress and contact pressure, and from that I would select the spring for the wear experiment. In order to finish the experiment in time, I had to select the spring prior to finishing the FE model. It would be ideal to test several springs as well to get a better comparison and let the wear experiment

run the full $5x10^6$ cycles, which would better differentiate the wear distribution and values. The linear wear differences in my case are very small, which could also be caused by the smaller amount of cycles. Further inaccuracies could occur in surface scanning and scan alignment, which is why it is difficult to make conclusions from the obtained results The proposed research would be time-wise long, but since other authors [83,84] have highlightened the importance of proper alignment and my own results also hint on the relationship between proper balancing and implant wear, it would be helpful for further implant and surgical technique improvement, especially since there is no comparable research available.

Conclusion

The aim of my diploma thesis was to evaluate the impact of ligament balancing on implant life time. Ligament balancing is considered to be one of the key parts of a succesfull total knee replacement, but there are several possible techniques to choose from and the correct balancing highly depends on the experience of the surgeon. The wear of unbalanced implants, which directly relates to the final life time, has been described as an issue, but has not been studied yet.

The theoretical part provides an insight into the topics of knee anatomy and biomechanics, which are crucial for understanding the topic of ligament balancing. A brief review of knee implants and materials used for these replacements is presented as well. The ligament balancing term is described and several techniques, which are generally used by surgeons, are mentioned. Tribology and wear mechanisms are also presented, since linear wear is one of the evaluated parameters.

The practical part includes two experiments, each of these was conducted in a balanced and unbalanced state. The first is a finite element model of the knee implant, where one simulation included two opposing forces to represent the extra torque in the unbalanced state. This torque was estimated based on literature research. The creation and setup of the model are described, as well as the loading and displacement. Afterwards an actual knee replacement wear test, which was loaded the same way as the FE model, is presented. Two tibial inserts were tested, with one simulation running with an added spring to simulate the unbalanced state of the implant. The spring had the same maximal force as the extra added forces in the FE model.

The linear wear values calculated from the FE model using Archards equation are comparable to the values obtained in the wear experiment. The highest calculated linear wear from the FE model in the unbalanced state was 0.197 mm (-3.43 % from the balanced state) for the lateral condyle and 0.156 mm (+40.54 % from the balanced state) for the medial condyle. This is comparable to the maximal 0.12 mm linear wear in the wear experiment, where no significant increase in linear wear was noted in the unbalanced state. The differences between the balanced and unbalanced linear wear values are small in both FE model and wear experiment, therefore it cannot be said that improper ligament balancing leads to shorter implant lifetimes.

References

(1) *Medical tribune: aktuální – nezávislá – mezinárodní*. Praha: Medical Tribune CZ, 2016, **2016**(11). ISSN 1214-8911.

(2) *Revizní operace TEP kyčlí a kolen* [online]. Pardubice, 2015 [cit. 2018-07-08]. Available at: http://pardubice.nempk.cz/ortopedie-revizni-operace-tep-kycli-kolen

(3) ČIHÁK, Radomír. Anatomie 1. 2., upr. a dopl. vyd. Praha: Grada Publishing, 2001, 497 s. ISBN 80-716-9970-5.

(4) Picture of Knee Joint. *Medicine Net* [online]. [cit. 2018-05-30]. Available at: https://www.medicinenet.com/image-collection/knee_joint_picture/picture.htm

(5) DYLEVSKÝ, Ivan. Pohybový systém – opěrná a nosná část. DYLEVSKÝ, Ivan, Rastislav DRUGA a Olga MRÁZKOVÁ. Funkční anatomie člověka. 1. vyd. Praha: Grada, 2000, s. 37-180. ISBN 80-7169-681-1.

(6) Knee Joint. In: *Medical Dictionary* [online]. 2009 [cit. 2018-10-25]. Available at: https://medical-dictionary.thefreedictionary.com/knee+joint

(7) Meniscus Anatomy, Function and Significance. *Bone and Spine* [online]. [cit. 2018-05-30]. Available at: http://boneandspine.com/meniscus-anatomy-function-and-significance/

(8) Knee Bursitis. In: *Rehab My Patient* [online]. [cit. 2018-10-25]. Available at: https://www.rehabmypatient.com/knee/knee-bursitis

(9) Muscles of the Knee. *Pro Knee Pain Relief* [online]. [cit. 2018-05-30]. Available at: http://prokneepainrelief.com/muscles-of-the-knee/

(10) The Importance of Training your legs. In: *Muscular Strength* [online]. [cit. 2018-10-25]. Available at: https://muscularstrength.com/article/The-Importance-Of-Training-Your-Legs-What-To-Know-About-Your-Bodys-Biggest-Muscle-Group

(11) *Hip Muscles* [online]. In: [cit. 2018-10-25]. Available at: https://www.easyflexibility.com/products/hip-combo-3-advanced-level

(12) ČIHÁK, Radomír. Anatomie 3. 2., upr. a dopl. vyd. Praha: Grada Publishing, 2004, 673 s. ISBN 80-247-1132-X.

(13) BARTONÍČEK, J., HEŘT, J. Základy klinické anatomie pohybového aparátu. Praha: Maxdorf, 2004, 256 s. ISBN 80-734-5017-8.

(14) *Blood Supply To The Foot* [online]. In: [cit. 2018-10-25]. Available at: https://www.orthobullets.com/foot-and-ankle/12114/blood-supply-to-the-foot

(15) CHHABRA, A., ELLIOTT, C. C., MILLER, M. D. (2001). Normal anatomy and biomechanics of the knee. Sports Medicine & Arthroscopy Review, 9(3), 166–177.
(16) FLANDRY, F., HOMNIEL, G. (2011). Normal anatomy and biomechanic of the knee. Sports Medicine & Arthroscopy Review, 19(2), 82–92.
(17) KOMDEUR, P., POLLO, F.E., JACKSON, R.W. Dynamic knee motion in anterior cruciate impairment: a report and case study. *Proceedings (Baylor University Medical Center)*. 2002;15(3):257-259.
(18) KAPANDJI, I. A. (1987). The Physiology of the joints. Volume two – The lower limb. New York: Churchill – Livingstone.
(19) LEVANGIE, P. K., NORKIN, Cynthia C. *Joint structure and function: a comprehensive analysis*. 2nd ed. Philadelphia, PA: F.A. Davis Co., c1992.
(20) BEZNOSKA, S., ČECH, O, LÖBL, K. Umělé náhrady lidských kloubů: biomechanické, materiálové a technologické aspekty., 1. vyd. Praha: Státní nakladatelství technické literatury, 1987, 246 s.
(21) BARTONÍČEK, J., ČECH, O., SOSNA, A.: Poranění vazivového aparátu kolenního kloubu. Praha, Avicenum, 1986
(22) *UNIT VII – The Knee* [online]. Virginia Commonwealth Unviersity [cit. 2018-07-09]. Available at:https://courses.vcu.edu/DANC291-003/index_7.htm
(23) KRAJÍČEK, Tomáš. *Fyzioterapie po plastice ligamentum crutiatum anterius*. Brno, 2006. Bachelor Thesis. Univerzita Karlova v Praze, 2.lékařská fakulta.
(24) EDITED BY OTTO RUSSE. *An atlas of examination, standard measurements and diagnosis in orthopedics and traumatology*. 2nd ed. Bern: H. Huber, 1972. ISBN 9783456001685.
(25) ŠKOLNÍKOVÁ, B.: Komplexná rehabilitačná ličba po úrazoch měkkého kolena v NRC Kováčová. Rehabilitácia, 33(1), 2000, s. 28-42
(26) NÝDRLE, M., VESELÁ, H.: Jedna kapitola ze speciální rehabilitace poranění kolenního kloubu. Brno, IDVPZ, 1992
(27) DYLEVSKÝ, I., KUBÁLKOVÁ, L., NAVRÁTIL, L.: Kineziologie, kinezioterapie a fyzioterapie. Praha, Manus, 2001
(28) Ligament instability in the knee. *Ottobock* [online]. 2015 [cit. 2018-07-10]. Available at: https://www.ottobock.com.au/orthotics/clinical-pictures-and-symptoms/ligament-laxity-knee/
(29) MAYER, M., SMÉKAL, D.: Měkké struktury kolenního kloubu a poruchy motorické kontroly. Rehabilitace a fyzikální lékařství, č. 3, 2004, s.111-117

(30) AGEBERG, E: Consequences of ligament injury on neuromuscular function and relevance to rehabilitation – using the anterior cruciate ligament-injured knee as model. J. electromyography kinesiol., 12, 2002, s.205-212

(31) WOJTYS, E. M., HUSTON, L. J: Longitudinal Effects of Anterior Cruciate Ligament Injury and Patellar Tendon Autograft Reconstruction on Neuromuscular Performance [Abstract]. Am. J. Sports Med., 28, 2000, s. 336-344

(32) BRUHN, S., GOLLHOFFER, A., GRUBER, M.: Proprioception training for prevention and rehabilitation of knee joint injurie [Abstract]. Eur. J. Sports Traumatol., Rel. Res., 23, 2001, s. 82-89

(33) Masarykova univerzita. Kinematická navigace v kolenní edoprotetice [online]. [cit.2018-05-19]. Available at: https://is.muni.cz/th/18777/lf_d/Kinematicka_navigace_v_kolenni_endoprotetice.txt

(34) RYBKA, V., VAVŘÍK, P. Aloplastika kolenního kloubu. 1. vyd. Praha: ARCADIA s.r.o., 1993. ISBN 80-901423-9-7

(35) ZDĚBLO, J. Totální endoprotéza kolenního kloubu, Brno: Vysoké učení technické v Brně, Fakulta strojního inţenýrství, 2011. 59 s. Vedoucí bakalářské práce Ing. Zdeněk Florian, CSc.

(36) KOKUBO, Tadashi. Bioceramics and their clinical applications. 1. vyd. Abington: Woodhead Publishing Limited, 2008. ISBN 978-1-84569-204-9.

(37) BEZNOSKA, S., ČECH, O., LÖBL, K.: Umělé náhrady lidských kloubů, Biomechanické, materiálové a technologické aspekty, Praha: SNTL – Nakladatelství technické literatury, n.p.

(38) PTÁČEK, L. a kolektiv: Nauka o materiálu I., Brno: Akademické nakladatelství CERM, s.r.o. ISBN: 80-7204-283-1

(39) PTÁČEK, L. a kolektiv: Nauka o materiálu II., Brno: Akademické nakladatelství CERM, s.r.o. ISBN: 80-7204-248-3

(40) Taking a PEEK at the future of replacement knee joints. *Medical Technologies* [online]. 2014 [cit. 2018-10-25]. Available at: http://medical-technologies.leeds.ac.uk/case-study/taking-a-peek-at-the-future-of-replacement-knee-joints/

(41) POKORNÝ, D., ŠLOUF, M., FULÍN, P. Současné poznatky o vlivu technologie výroby a sterilizace na strukturu, vlastnosti a životnost UHMWPE v kloubních náhradách. In: *Acta chirurgiae orthopaedicae et traumatologiae*. 79,2012, p. 213-221.

(42) Tiibial insert. In: *Omnia* [online]. [cit. 2019-05-11]. Available at: https://www.omniagmd.com/product/tibial-insert

(43) ŠLOUF, M., FENCL, J., POKORNÝ, D., FULÍN, P. Nové typy a generace UHMWPE pro kloubní náhrady. *REVIEW*. (1/2013).

(44) AOX Antioxidant Polyethylene. *DePuySynthes* [online]. [cit. 2019-05-11]. Available at: http://synthes.vo.llnwd.net/o16/LLNWMB8/US%20Mobile/Synthes%20North%20America/Product%20Support%20Materials/Brochures/DSUS-JRC-0714-0314%20AOX.pdf

(45) PRUDHON, J.L., Verdier, R. Cemented or cementless total knee arthroplasty?. *SICOT-J* [online]. 2017, **3**, 70- [cit. 2018-07-10]. DOI: 10.1051/sicotj/2017046. ISSN 2426-8887. Available at: http://www.sicot-j.org/10.1051/sicotj/2017046

(46) MILLER, Adam J. Results of Cemented vs Cementless Primary Total Knee Arthroplasty Using the Same Implant Design. *The Journal of Arthroplasty* [online]. **33**(4), 1089-1093 [cit. 2018-07-10].

(47) *Hip Joint Replacement Surgery* [online]. In: . [cit. 2018-10-25]. Available at: https://www.healthpages.org/surgical-care/hip-joint-replacement-surgery/

(48) MATASSI, F., CARULLI, C., CIVININI, R., INNOCENTI, M. Cemented versus cementless fixation in total knee arthroplasty. *Joints*. 2014;1(3):121-5. Published 2014 Jan 8.

(49) JAROSLAV, M. Zdravotnické noviny: Rehabilitační problematika kolenních náhrad (Hlavní téma: Endoprotetika kolene), 2003, roč. 52, č. 23, s. 8-17. ISSN: 1214-7664

(50) KOVÁŘÍKOVÁ, Adéla. *Analýza adhezních zkoušek kolagenové nanovrstvy na implantátu*. Praha, 2017. Bakalářská práce. České vysoké učení technické v Praze.

(51) DUNGL, P. – PAVLANSKÝ, R. – PODŠKUBKA, A. Acta chirurgiae orthopaedicae et traumatologiae čechoslovaca: Naše zkušenosti s aloplastikou kolenního kloubu, 1982, roč. 49, č. 1, s. 49-62. ISSN: 0001-5415

(52) MAJVALD, Jiří. *BIOMECHANICKÁ STUDIE TEP KOLENNÍHO KLOUBU A ALTERNATIVY K JEJÍ IMPLANTACI*. Brno, 2014. Bachelor Thesis. Vysoké Učení Technické v Brně.

(53) Knee Endoprosthesis. *Beznoska* [online]. [cit. 2018-05-30]. Available at: http://www.beznoska.com/product/hinge-rotation-knee-endoprosthesis-type-cms/

(54) Three-Compartment Knee Prosthesis. *Medical EXPO* [online]. [cit. 2018-05-30]. Available at: http://www.medicalexpo.com/prod/corin/product-80816-623455.html

(55) MOZELLA, Alan de Paula, Felipe BORGES GONÇALVES, Jansen OSTERNO VASCONCELOS a Hugo Alexandre DE ARAÚJO BARROS COBRA. Revisão de artroplastia unicompartimental de joelho: implantes usados e causas de falha. *Revista Brasileira de Ortopedia*[online]. 2014, **49**(2), 154-159 [cit. 2018-07-10]. DOI: 10.1016/j.rbo.2014.02.002. ISSN 01023616. Available at: http://linkinghub.elsevier.com/retrieve/pii/S010236161400037X

(56) Unicondylar/ Unicomplartmental / Partial Knee Replacement. *Indiamart*[online]. [cit. 2018-05-30]. Available at: https://www.indiamart.com/proddetail/unicondylar-unicompartmental-partial-knee-replacement-15436791291.html

(57) BABAZADEH, Sina. The relevance of ligament balancing in total knee arthroplasty: how important is it? A systematic review of the literature. *Orthopedic Reviews* [online]. 2009, **1**(1), 26- [cit. 2018-05-31]. DOI: 10.4081/or.2009.e26. ISSN 2035-8164. Available at: http://www.pagepress.org/journals/index.php/or/article/view/or.2009.e26

(58) AHN, Ji Hyun. Comparative Study of Two Techniques for Ligament Balancing in Total Knee Arthroplasty for Severe Varus Knee: Medial Soft Tissue Release vs. Bony Resection of Proximal Medial Tibia [online]. 2013. [cit. 2018-05-31]. Available at: http://www.jksrr.org/journal/view.html?doi=10.5792/ksrr.2013.25.1.13

(59) Knee Ligaments and Other Knee Stabilizers. *Bone and Spine* [online]. [cit. 2018-05-30]. Available at: http://boneandspine.com/knee-ligaments-and-other-knee-stabilizers/

(60) UNITT, L., A. SAMBATAKAKIS, D. JOHNSTONE a T. W. R. BRIGGS. Short-term outcome in total knee replacement after soft-tissue release and balancing. *The Journal of Bone and Joint Surgery. British volume*[online]. 2008, **90-B**(2), 159-165 [cit. 2018-05-31]. DOI: 10.1302/0301-620X.90B2.19327. ISSN 0301-620X. Available at: http://online.boneandjoint.org.uk/doi/10.1302/0301-620X.90B2.19327

(61) *Diagram of Knee Ligaments* [online]. [cit. 2018-05-30]. Available at: http://www.jugosparabajardepeso.info/organdiagram/2844-2845

(62) ROSSI, Roberto, Federica ROSSO, Umberto COTTINO, Federico DETTONI, Davide Edoardo BONASIA a Matteo BRUZZONE. Total knee arthroplasty in the valgus knee. *International Orthopaedics* [online]. 2014, **38**(2), 273-283 [cit. 2018-07-10]. DOI: 10.1007/s00264-013-2227-4. ISSN 0341-2695. Available at: http://link.springer.com/10.1007/s00264-013-2227-4

(63) *Current surgical strategies for total arthroplasty in valgus knee* [online]. In: . [cit. 2018-10-25]. Dostupné z: https://www.wjgnet.com/2218-5836/full/v6/i6/469.htm

(64) Valgus vs. Varus. *All Health Post* [online]. [cit. 2018-05-30]. Available at: https://allhealthpost.com/valgus-vs-varus/

(65) Stribeck curve. In: *Wikipedia: the free encyclopedia* [online]. San Francisco (CA): Wikimedia Foundation, 2001- [cit. 2019-05-11]. Available at: https://en.wikipedia.org/wiki/Stribeck_curve

(66) Lubrication. In: *Wikipedia: the free encyclopedia* [online]. San Francisco (CA): Wikimedia Foundation, 2001- [cit. 2019-05-11]. Available at: https://en.wikipedia.org/wiki/Lubrication#Lubrication_Regimes

(67) Stribeck curve during liquid lubrication. In: *Reasearch Gate* [online]. [cit. 2019-05-11]. Available at: https://www.researchgate.net/figure/Stribeck-curve-during-liquid-lubrication_fig1_321317529

(68) *ISO 14234-3:2002 Implants for surgery – Wear of total knee-joint prostheses*. 15.9.2004.

(69) GAO, Yongchang, Jing ZHANG and ZHONGMIN Jin. "Explic it finite element modeling of kinematics and contact mechanics of artificial hip and knee joints." (2015).

(70) Dynamic Finite Element Analysis of Mobile Bearing Type Knee Prosthesis under Deep Flexional Motion. *The Scientific World Journal* [online]. [cit. 2019-05-11]. Available at: https://www.hindawi.com/journals/tswj/2014/586921/

(71) EN 1.4301 (X5CrNi18-10) Stainless Steel. *MakeItFrom.com* [online]. [cit. 2019-07-10]. Available at: https://www.makeitfrom.com/material-properties/EN-1.4301-X5CrNi18-10-Stainless-Steel

(72) UNS R30075 (ASTM F75, ISO 5832-4) Co-Cr-Mo Alloy. *MakeItFrom.com* [online]. [cit. 2019-07-10]. Available at: https://www.makeitfrom.com/material-properties/UNS-R30075-ASTM-F75-ISO-5832-4-Co-Cr-Mo-Alloy

(73) TARNITA, Daniela & Marian CALAFETEANU, Dan & Geonea, Ionut & Petcu, Alin & Tarnita, Danut. (2017). Effects of malalignment angle on the contact stress of knee prosthesis components, using finite element method. Romanian journal of morphology and embryology = Revue roumaine de morphologie et embryologie. 58. 831-836.

(74) LIU, F., GALVIN, A., JIN, Z., & FISHER, J. (2011). A New Formulation for the Prediction of Polyethylene Wear in Artificial Hip Joints. *Proceedings of the Institution of Mechanical Engineers, Part H: Journal of Engineering in Medicine*, *225*(1), 16–24. https://doi.org/10.1243/09544119JEIM819

(75) Totální náhrada kolenního kloubu typ SVL/SVS. In: *Beznoska s.r.o.* [online]. [cit. 2019-06-17]. Available at: http://www.beznoska.cz/product/totalni-nahrada-kolenniho-kloubu-typ-svlsvs/

(76) Optický 3D souřadnicový stroj RedLux. In: *Laboratoř biomechaniky člověka* [online]. [cit. 2019-05-11]. Available at: http://www.biomechanika.cz/projects/77?category_id=30

(77) Simulator KKK ELO 2011. [online]. [cit. 2019-05-11]. Available at: http://www.biomechanika.cz/deparments/25

(78) Primary, Double, and Triple Varus Knee Syndromes: Diagnosis, Osteotomy Techniques, and Clinical Outcomes[online]. 2016 [cit. 2019-02-10]. Available at: https://musculoskeletalkey.com/primary-double-and-triple-varus-knee-syndromes-diagnosis-osteotomy-techniques-and-clinical-outcomes/

(79) DELL'ISOLA, A., S.L. SMITH, M.S. ANDERSEN a M. STEULTJENS. Knee internal contact force in a varus malaligned phenotype in knee osteoarthritis (KOA). Osteoarthritis and Cartilage [online]. 2017, 25(12), 2007-2013 [cit. 2019-02-10]. DOI: 10.1016/j.joca.2017.08.010. ISSN 10634584. Available at: https://linkinghub.elsevier.com/retrieve/pii/S1063458417311573

(80) MOOTANAH, R., C.W. IMHAUSER, F. REISSE, et al. Development and validation of a computational model of the knee joint for the evaluation of surgical treatments for osteoarthritis. Computer Methods in Biomechanics and Biomedical Engineering [online]. 2013, 17(13), 1502-1517 [cit. 2019-02-10]. DOI: 10.1080/10255842.2014.899588. ISSN 1025-5842. Available at: http://www.tandfonline.com/doi/abs/10.1080/10255842.2014.899588

(81) NAKAMURA, S., Y. TIAN, Y. TANAKA, S. KURIYAMA, H. ITO, M. FURU a S. MATSUDA. The effects of kinematically aligned total knee arthroplasty on stress at the medial tibia. Bone & Joint Research [online]. 2017, 6(1), 43-51 [cit. 2019-02-10]. DOI: 10.1302/2046-3758.61.BJR-2016-0090.R1. ISSN 2046-3758. Available at: http://online.boneandjoint.org.uk/doi/10.1302/2046-3758.61.BJR-2016-0090.R1

(82) Tlačné pružiny z pružinové oceli. In: *Hennlich* [online]. [cit. 2019-06-18]. Available at: https://www.hennlich.cz/produkty/pruziny-tlacne-pruziny-162/tlacne-pruziny-z-pruzinove-oceli.html

(83) INGRASSIA, T., L. NALBONE, V. NIGRELLI, D. TUMINO a V. RICOTTA. Finite element analysis of two total knee joint prostheses. International Journal on Interactive Design and Manufacturing (IJIDeM) [online]. 2013, 7(2), 91-101 [cit.

2019-08-02]. DOI: 10.1007/s12008-012-0167-7. ISSN 1955-2513. Available at: http://link.springer.com/10.1007/s12008-012-0167-7

(84) SUH, D-S., K-T. KANG, J. SON, O-R. KWON, C. BAEK a Y-G. KOH. Computational study on the effect of malalignment of the tibial component on the biomechanics of total knee arthroplasty. Bone & Joint Research [online]. 2017, 6(11), 623-630 [cit. 2019-08-02]. DOI: 10.1302/2046-3758.611.BJR-2016-0088.R2. ISSN 2046-3758. Available at: http://online.boneandjoint.org.uk/doi/10.1302/2046-3758.611.BJR-2016-0088.R2

(85) SHI, Junfen. Finite element analysis of total knee replacement considering gait cycle load and malalignment. Wolverhampton, 2007. Doctoral Thesis. University of Wolverhampton.

List of Figures